Molecular Therapy
Original Article

Targeting of Aberrant αvβ6 Integrin Expression in Solid Tumors Using Chimeric Antigen Receptor-Engineered T Cells

Lynsey M. Whilding,[1] Ana C. Parente-Pereira,[1] Tomasz Zabinski,[1] David M. Davies,[1] Roseanna M.G. Petrovic,[1] Y. Vincent Kao,[1] Shobhit A. Saxena,[1] Alex Romain,[1] Jose A. Costa-Guerra,[1] Shelia Violette,[2] Hiroaki Itamochi,[3] Sadaf Ghaem-Maghami,[4] Sabari Vallath,[5] John F. Marshall,[5] and John Maher[1,6,7]

[1]King's College London, King's Health Partners Integrated Cancer Centre and Division of Cancer Studies, Guy's Hospital, Great Maze Pond, London SE1 9RT, UK; [2]Biogen Idec, Cambridge, MA 02142, USA; [3]Department of Obstetrics and Gynecology, Iwate Medical University School of Medicine, Iwate 020-8505, Japan; [4]Department of Surgery and Cancer, Imperial College London, Hammersmith Hospital, Du Cane Road, London W12 0NN, UK; [5]Centre for Tumour Biology, John Vane Science Centre, Barts Cancer Institute, Queen Mary University of London, Charterhouse Square, London EC1M 6BQ, UK; [6]Department of Clinical Immunology and Allergy, King's College Hospital NHS Foundation Trust, Denmark Hill, London SE5 9RS, UK; [7]Department of Immunology, Eastbourne Hospital, Kings Drive, Eastbourne, East Sussex BN21 2UD, UK

Expression of the αvβ6 integrin is upregulated in several solid tumors. In contrast, physiologic expression of this epithelial-specific integrin is restricted to development and epithelial re-modeling. Here, we describe, for the first time, the development of a chimeric antigen receptor (CAR) that couples the recognition of this integrin to the delivery of potent therapeutic activity in a diverse repertoire of solid tumor models. Highly selective targeting αvβ6 was achieved using a foot and mouth disease virus-derived A20 peptide, coupled to a fused CD28^{+}CD3 endodomain. To achieve selective expansion of CAR T cells ex vivo, an IL-4-responsive fusion gene (4αβ) was co-expressed, which delivers a selective mitogenic signal to engineered T cells only. In vivo efficacy was demonstrated in mice with established ovarian, breast, and pancreatic tumor xenografts, all of which express αvβ6 at intermediate to high levels. SCID beige mice were used for these studies because they are susceptible to cytokine release syndrome, unlike more immune-compromised strains. Nonetheless, although the CAR also engages mouse αvβ6, mild and reversible toxicity was only observed when supra-therapeutic doses of CAR T cells were administered parenterally. These data support the clinical evaluation of αvβ6 re-targeted CAR T cell immunotherapy in solid tumors that express this integrin.

INTRODUCTION

Adoptive immunotherapy using chimeric antigen receptor (CAR)-engineered autologous T cells has achieved unprecedented efficacy in the treatment of patients with refractory B cell malignancy.[1–3] In this context, the CD19 molecule provides a target par excellence, since toxicity arising from the depletion of healthy B cells can be mitigated with immunoglobulin replacement therapy. However, solid tumors present several additional hurdles to the development of effective CAR T cell immunotherapy. Unlike B cell malignancy, lineage-restricted molecules are generally unsuitable for targeting owing to their expression at high levels by one or more critical organs. Broadly speaking, two alternative approaches warrant consideration. First, tumor-specific mutations (e.g., epidermal growth factor receptor variant III) provide attractive opportunities for immunotherapy of selected cancers.[4,5] However, target expression is sporadic, subject to intra-tumoral heterogeneity and downregulation upon disease relapse.[6,7] Alternatively, targeting may be directed against molecules that are overexpressed on transformed cells relative to healthy tissue, such as ErbB2. While initial clinical testing resulted in lethal toxicity,[8] more recent evaluation of this strategy has demonstrated that an efficacy signal can be achieved safely using CAR^{+} T cells.[9] This provides a strong rationale for the identification and validation of additional targets that are not absolutely tumor specific but that are strongly upregulated on transformed cells and contribute to disease pathogenesis.

One such candidate is the epithelial-specific integrin αvβ6. Cell surface expression requires pairing of the monogamous β6 chain with the more promiscuous αv partner.[10] αvβ6 is commonly overexpressed in solid tumors derived from pancreas, head and neck, skin, lung, esophagus, stomach, colon, breast, uterine cervix, and fallopian tube/ovary, and it is generally associated with worsened prognosis.[11–17] In keeping with this, αvβ6 activates pro-transforming growth factor β and promotes epithelial-to-mesenchymal transition, cellular migration, and matrix metalloproteinase activity.[18–21] By contrast, this integrin is minimally expressed in adult tissue, except during wound healing.[17,22] In light of these attributes, αvβ6 has attracted significant interest as a target for antibody-based imaging and treatment of many cancer types.[14,23,24]

Received 9 June 2016; accepted 6 October 2016;
http://dx.doi.org/10.1016/j.ymthe.2016.10.012.

Correspondence: John Maher, Division of Cancer Studies, Guy's Hospital, Third floor Bermondsey Wing, Great Maze Pond, London SE1 9RT, UK.
E-mail: john.maher@kcl.ac.uk

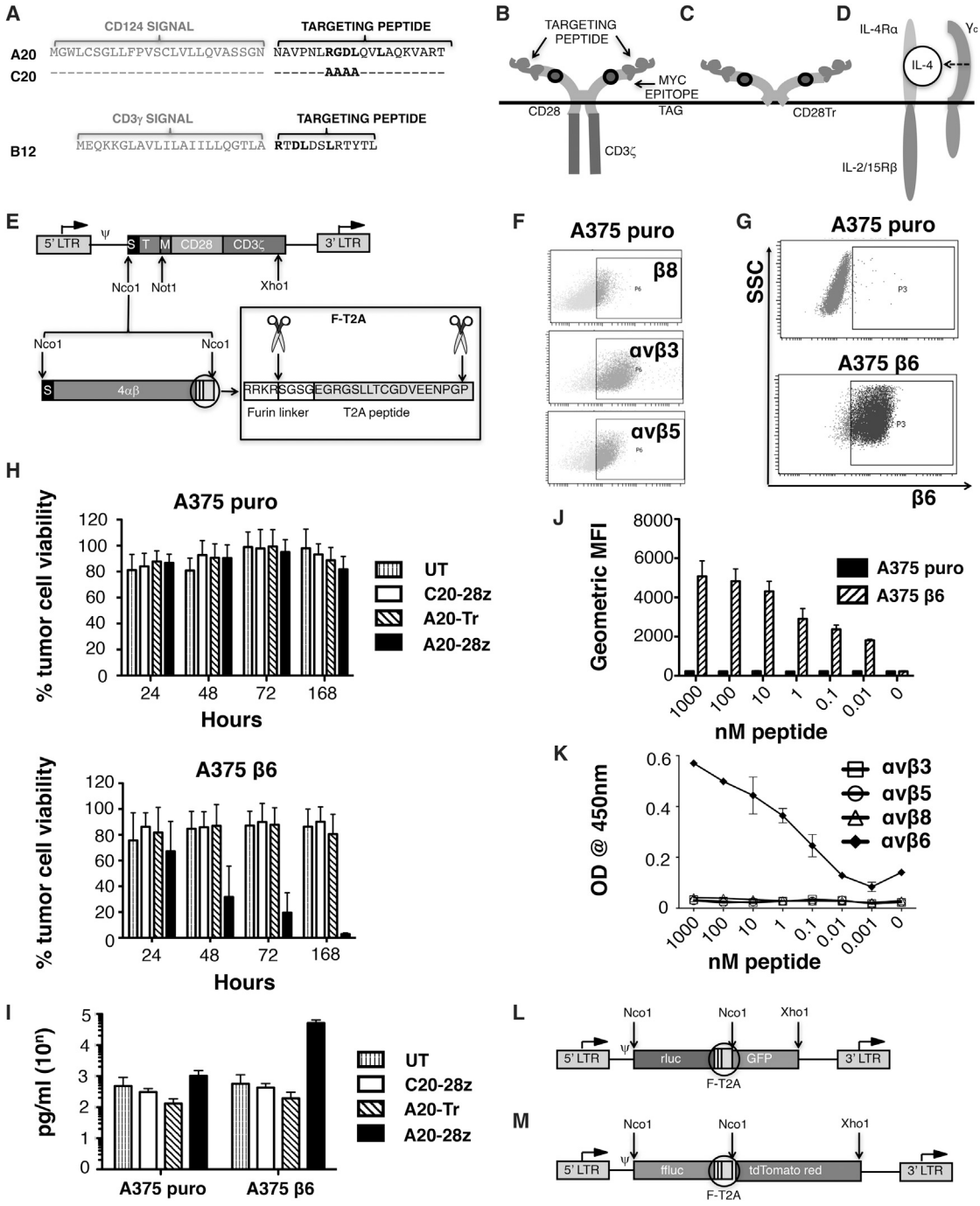

Figure 1. Design and Integrin Specificity of Retroviral-Encoded CAR Constructs

(A) To create an αvβ6-specific CAR-targeting moiety, the A20 peptide derived from the GH loop of the capsid protein VP1 from foot and mouth disease virus (serotype 01 BFS) was placed downstream of a CD124 signal peptide. A matched but scrambled peptide (named C20) was generated in which RGDL was replaced with AAAA. A second αvβ6-specific CAR-targeting moiety was engineered by placing the B12 peptide downstream of a CD3γ signal peptide. (B) Schematic structures show αvβ6-specific CARs and (C) matched endodomain-truncated control. (D) Schematic structure shows 4αβ chimeric cytokine receptor in which the IL-4 receptor α ectodomain is fused to the transmembrane and endodomain of the shared IL-2/15 receptor β. (E) The SFG retroviral vector was used to express CARs in human T cells. LTR, long terminal repeat; S, signal peptide; T, targeting moiety; M, human c-*myc* epitope tag, recognized by 9e10 antibody. In some constructs, equimolar co-expression of the IL-4-responsive 4αβ chimeric cytokine receptor was achieved using a *Thosea Asigna* (T)2A ribosomal skip peptide, placed downstream of a furin cleavage site, designed to remove peptide overhangs on the C terminus of the upstream encoded polypeptide. (F) Expression of the indicated integrins in A375 cells as detected by flow cytometry is shown. (G) A375 cells were

(legend continued on next page)

Infection of several species by the foot and mouth disease virus (FMDV) is mediated by the ability of the viral protein 1 coat protein to bind to a number of integrins, including αvβ6.[25] A derived 20-mer peptide (A20FMDV2) has been characterized as an effective antagonist of αvβ6[26] and has been used to image αvβ6-positive tumors.[27] We hypothesized that this 20-mer would represent a suitable moiety to engineer an αvβ6-targeted CAR, since it contains two overlapping αvβ6-binding motifs (RGD and DLXXL) and binds with >1,000-fold greater specificity to this integrin than to other family members, such as αvβ3, αvβ5, and α5β1.[13,28] Using A20FMDV2 as a targeting moiety, we describe for the first time the development of an αvβ6-specific CAR that elicits potent therapeutic activity against diverse solid tumor types, without significant toxicity.

RESULTS

αvβ6 Integrin Is Expressed by Cell Lines Derived from Multiple Solid Tumors

Figure S1 shows αvβ6 expression by the panel of human tumor cells used in this study. High-level expression (100% positive; geometric mean fluorescence intensity [MFI] >2,000) was found in pancreatic ductal adenocarcinoma (PDAC) cell lines (Panc0403, BxPC3), in BT20 triple-negative breast cancer (TNBC) cells, and in the clear cell epithelial ovarian carcinoma (EOC) cell line OVSAYO. Intermediate expression (MFI 1,000–2,000) was observed in the PDAC cell line CFPAC1; the TNBC cell line MDA-MB-468; and in the SKOV-3, OVMANA, TUOC1, and OVTOKO EOC cell lines. Lower expression (MFI 150–999) was detected in luminal (T47D, MCF7, and ZR75) and luminal/HER2$^+$ (BT474) breast cancer cells and in the OVSAHO, HAC2, SMOV2, OVAS, and KK EOC cell lines. Minimal expression (MFI <150; $\leq$9%$^+$ events) was found in the PDAC cell line Panc-1; the TNBC cell line CAL51; and in the A2780, A2780CP, Kuramochi, and TOV21G EOC cell lines.

Comparison of In Vitro Anti-tumor Activity of Candidate αvβ6-Targeted CARs

To engineer candidate αvβ6 CARs, the A20FMDV2 peptide (A20)[26] or a phage display-derived 12-mer peptide (B12)[29] was fused to a human CD28 spacer (from amino acid 114, in which MYPPPY was replaced by a 9e10 myc tag), followed by a CD28 transmembrane/endodomain and a CD3ζ endodomain. CARs were named A20-28z and B12-28z and contained two or one αvβ6-binding site, respectively (Figures 1A and 1B). A scrambled derivative of A20 (C20, in which RGDL is replaced by AAAA; Figure 1A) or truncated CD28 endodomain (Figure 1C) were used to create control CARs (named C20-28z and A20-Tr, respectively)[30] (Figures 1B and 1C). CARs were stoichiometrically co-expressed using a *Thosea Asigna* (T)2A peptide-containing vector, with a chimeric cytokine receptor 4αβ (Figure 1D) to enable preferential expansion of αvβ6-re-targeted T cells ex vivo. All CARs were delivered to human T cells using the SFG retroviral vector (Figure 1E).

To compare function, human CAR T cells were co-cultivated with PDAC tumor cells that naturally express minimal (min; Panc-1), intermediate (CFPAC1), or high levels of αvβ6 (Panc0403, BxPC3). A20-28z$^+$ T cells released large quantities of interferon (IFN)-γ when co-cultivated with αvβ6$^+$ PDAC cells, accompanied by tumor cell killing, monolayer destruction, and enrichment of transduced T cells following CAR stimulation (Figure S2). By contrast, cytotoxic activity of B12-28z$^+$ T cells was minimal or absent, and it was unaccompanied by reproducible cytokine release or CAR T cell enrichment following stimulation (Figure S2; data not shown).

In light of these findings, A20-28z was advanced and B12-28z was discarded. Specificity of integrin targeting was evaluated in cytotoxicity assays using A375 cells that naturally express several RGD-binding integrins, including αvβ3, αvβ5, αvβ8, and α5β1, but not αvβ6 (Figures 1F and 1G).[24] Comparison was made with cytotoxicity against a β6$^+$ A375 derivative (Figure 1G). In an extended cytotoxicity assay that lasted 1–7 days, A20-28z$^+$ T cells killed β6$^+$, but not control, A375 cells (Figure 1H), accompanied by β6-dependent IFN-γ release (Figure 1I). As expected, neither A20-Tr$^+$ nor C20-28z$^+$ T cells demonstrated cytotoxic activity in these assays. To further characterize the specificity of the A20 peptide, its binding capacity for other integrins also was assessed. The addition of increasing amounts of biotinylated A20 peptide led to proportionately greater binding to both A375 β6 cells (Figure 1J) and to recombinant αvβ6 (Figure 1K). By contrast, the A20 peptide did not exhibit any detectable binding to A375 puro cells or to other RGD-binding integrins (Figures 1J and 1K).

Expansion of αvβ6-Re-targeted T Cells Using Interleukin-4

To preferentially expand αvβ6-re-targeted T cells ex vivo, CARs were stoichiometrically co-expressed using a *Thosea Asigna* (T)2A peptide-containing vector with 4αβ (Figure 1E). The 4αβ chimeric cytokine receptor comprises the human IL-4 receptor α ectodomain, which has been fused to the shared human IL-2/IL-15 receptor β transmembrane and endodomain regions. Binding of the poorly

transduced with the pBabe puro retroviral vector (A375 puro) or with pBabe puro that encodes for the integrin β6 subunit. Cell surface expression of β6 was determined in both cell populations by flow cytometry. SSC, side scatter. (H) A375 puro cells (αvβ6 negative) or A375 β6 cells (αvβ6 positive) were co-cultivated at a 1:1 ratio with the indicated CAR-engineered T cells in the absence of exogenous cytokine. Data show the mean ± SD of residual tumor cell viability from five independent experiments, each performed in triplicate. Survival was quantified by MTT assay at 24–168 hr and expressed relative to untreated tumor cells (set at 100% viability). (I) Cells were co-cultivated at a 1:1 ratio with the indicated CAR-engineered T cells in the absence of exogenous cytokine for 48 hr. Data show the mean ± SD of IFN-γ detected in the cell supernatant from three independent experiments, each performed in duplicate. (J) Binding of biotinylated A20 peptide to A375 puro cells (αvβ6-negative) or A375 β6 cells (αvβ6-positive) was detected by flow cytometry. Data show the mean ± SD geometric mean fluorescent intensity of four independent experiments. (K) Binding of biotinylated A20 peptide to recombinant integrins was quantified by ELISA. (L) SFG rluc/GFP vector, which co-expresses *Renilla* luciferase (red-shifted 8.6-535 variant) with GFP using a furin-T2A (F-T2A)-intervening sequence, is shown. (M) SFG ffluc/tdTom vector, which co-expresses firefly luciferase with tdTomato red fluorescent protein using an F-T2A-intervening sequence, is shown.

mitogenic cytokine IL-4 leads to the delivery of a potent and selective growth signal in 4αβ$^+$ T cells.[31] Consequently, all 4αβ$^+$ CAR T cell populations underwent selective enrichment and expansion when cultured in IL-4 (Figure S3A). The addition of exogenous IL-4 significantly increased cytotoxicity of A20-28z/4αβ T cells against BxPC3 cells in vitro (Figure S3B), accompanied by a non-significant trend toward increased IFN-γ release (Figure S3C). Neither the co-expression of 4αβ nor the addition of IL-4 resulted in an alteration in the proportion of CAR T cells with naive (CCR7$^+$CD45RO$^-$), central memory (CCR7$^+$CD45RO$^-$), effector memory (CCR7$^-$CD45RO$^+$), or effector (CCR7$^-$CD45RO$^-$) phenotype, when compared to cells cultured in IL-2 (Figure S3D).

αvβ6-Re-targeted CAR T Cells Elicit Broad Anti-tumor Activity In Vitro

Following IL-4-mediated expansion in vitro, A20-28z/4αβ$^+$ and control C20-28z/4αβ$^+$ or A20-Tr/4αβ$^+$ T cells were evaluated for anti-tumor activity using a panel of cell lines that express varying levels of αvβ6. Unlike controls, A20-28z$^+$ T cells killed αvβ6$^+$ PDAC, HER2 amplified breast, luminal breast, TNBC, and ovarian tumor cells (Figures 2A–2E), accompanied by the release of IL-2 (Figure 3) and IFN-γ (Figure S4). Residual tumor cell viability and cytokine release correlated inversely or directly (respectively) with the intensity of αvβ6 expression on target cells (Figure 4). Importantly, however, tumor cells that expressed very low levels of αvβ6 (e.g., Panc-1 [Figure 2A] or CAL51 [Figure 2D]) were not killed.

avβ6-Re-targeted CAR T Cells Cause Regression of Several Tumor Xenografts with Minimal Toxicity

Firefly luciferase (ffluc)$^+$ SKOV-3 cells express αvβ6 and can be propagated as an intraperitoneal (i.p.) xenograft that is amenable to monitoring using bioluminescence imaging (BLI).[32] Consequently, this provides a convenient model to test in vivo anti-tumor activity of adoptively transferred αvβ6-re-targeted CAR T cells. To permit T cell imaging, co-transduction was performed with A20-28z/4αβ (or the control A20-Tr/4αβ retroviral vector) and a second retroviral vector that encodes for GFP and red-shifted *Renilla* luciferase (rluc; Figure 1L). After IL-4-mediated ex vivo enrichment for CAR T cell expression, transduced T cells were analyzed for the expression of CD8 and retroviral-encoded transgenes (Figure 5A). Functionality of CAR T cells was confirmed in vitro using cytotoxicity and cytokine release assays (data not shown) prior to i.p. transfer into severe combined immunodeficiency (SCID) beige mice with established SKOV-3 ffluc xenografts.

Mice treated with control A20-Tr/4αβ/rluc/GFP$^+$ CAR T cells or PBS had progressive disease. By contrast, mice treated with A20-28z/4αβ/rluc/GFP$^+$ CAR T cells exhibited tumor regression within 5 days of treatment, and they maintained a significantly lower tumor burden than either control group (Figures 5B and 5C). Treatment with αvβ6-re-targeted CAR T cells significantly extended median survival from 63 days (both control groups) to 82 days (A20-28z group; $p = 0.0014$) (Figure S5). Although the A20-28z CAR also can recognize αvβ6 expressed by murine cells, treatment was very well tolerated. Minimal weight loss (<5%) was observed in some mice, with complete resolution within 1 week (Figure 5D). This contrasts with severe weight loss and cytokine release syndrome (CRS) that may be induced in the same tumor xenograft model using ErbB-re-targeted CAR T cells.[33]

To investigate the generality of these findings, similar experiments were performed in which BxPC3 (Figure 6), MDA-MB-468 (Figure 7), or Panc0403 (Figure 8) tumor xenografts were established in SCID beige mice. As before, T cells were dual transduced to co-express rluc/GFP with A20-28z/4αβ or A20-Tr/4αβ and enriched for CAR$^+$ T cells by ex vivo culture in IL-4. Prior to adoptive transfer, T cells were analyzed for transgene expression (Figures 6A, 7A, and 8A) and for in vitro cytotoxicity and cytokine release following co-culture with αvβ6$^+$ tumor cells (data not shown). In all cases, mice treated with either PBS or A20-Tr/4αβ/rluc/GFP$^+$ T cells demonstrated similar levels of tumor progression, whereas A20-28z/4αβ/rluc/GFP$^+$ CAR T cells caused significant tumor regression (BxPC3, Figures 6B and 6C; MDA-MB-468, Figures 7B and 7C) or stabilization (Panc0403, Figure 8B), followed by delayed disease progression. Tumor regression was observed in the Panc0403 model in a second experiment, following treatment with A20-28z$^+$ T cells (Figure S6). Anti-tumor activity of αvβ6-re-targeted CAR T cells was associated with transient minor and fully reversible weight loss (Figures 6D, 7D, and 8C).

T Cell Imaging Demonstrates Inadequate Longevity of Human CAR T Cells in SCID Beige Mice

Engineering of CAR T cells to co-express rluc/GFP allowed serial monitoring of the bio-distribution of CAR T cells using BLI. It also provided quantitative information since we found that the number of CAR T cells present correlated directly with total flux (Figure S7). *Renilla* luciferase utilizes a different substrate (coelenterazine) than ffluc (d-luciferin), which is expressed by tumor cells in these models, allowing separate imaging of T cells and tumor in the same animals. Using this approach, we found that incomplete eradication of tumor burden correlated with progressive loss of CAR T cells following adoptive transfer, although a small residual population of CAR T cells was frequently detected (Panc0403 model; Figure 8D). Similar results were obtained in the SKOV-3 and BxPC3 models (data not shown). The administration of exogenous IL-4 exerted only a marginal impact on therapeutic activity when limiting numbers of CAR T cells were used to treat mice with advanced tumor burden (Figure S8A). This was accompanied by a non-significant trend toward delayed loss of CAR T cells in mice treated with high-dose IL-4 (Figure S8B). Combination treatment with CAR T cells and IL-4 was not toxic, indicated by the lack of weight loss in treated mice (Figure S8C).

Human CAR T Cells Recognize Mouse αvβ6, but They Cause Mild, Transient, and Fully Reversible Toxicity at Supra-therapeutic Dose Levels

The FMDV 20-mer also binds mouse αvβ6 with high affinity.[28] To test if human A20-28z$^+$ T cells engage the mouse αvβ6 ortholog, co-cultivation experiments were performed using 4T1 mammary

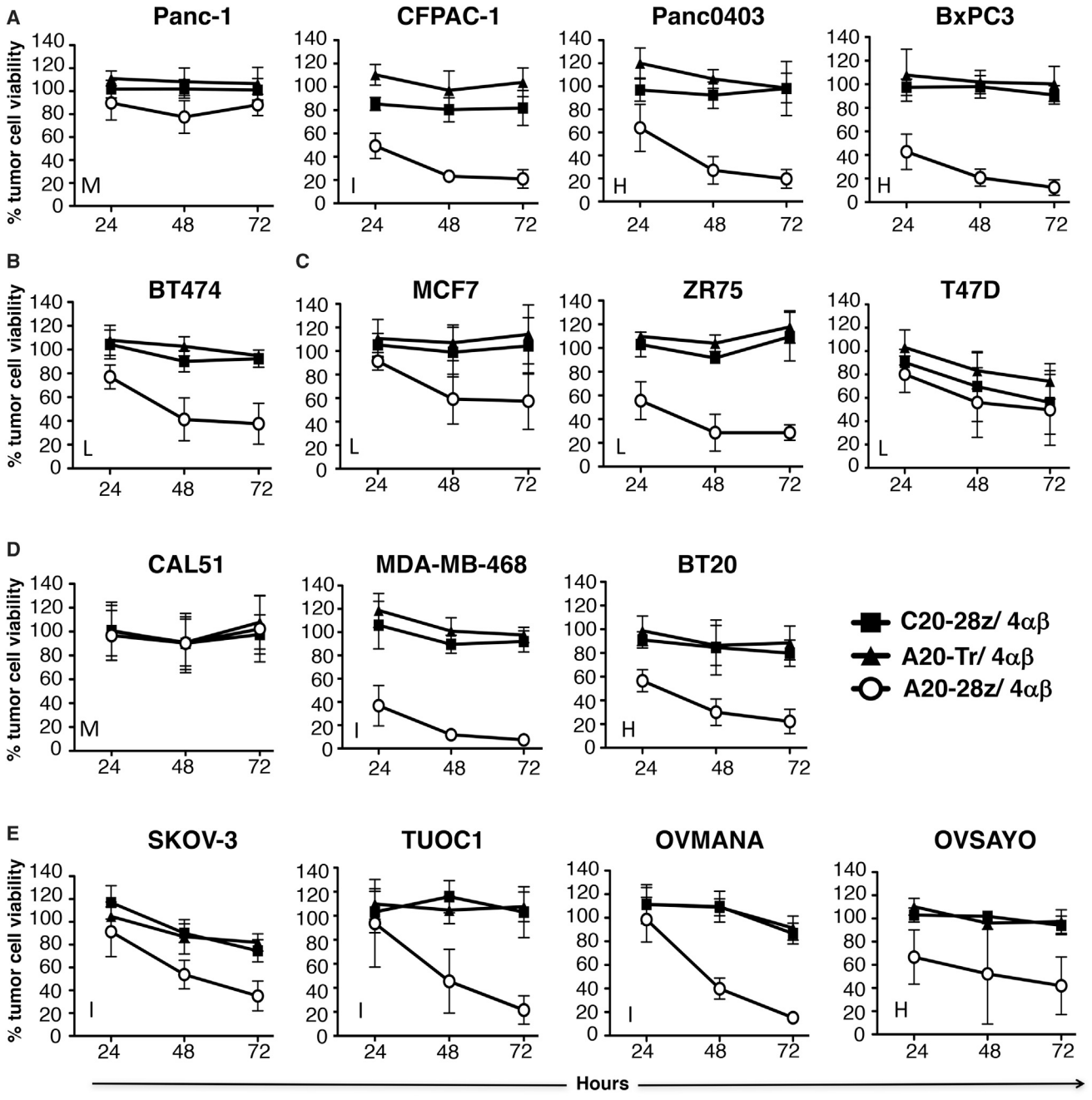

Figure 2. In Vitro Assessment of Anti-tumor Activity of CAR T Cells Targeted against αvβ6

Firefly luciferase-expressing pancreatic (A), HER2 amplified breast (B), luminal breast (C), triple-negative breast (D), or ovarian tumor cells (E) were co-cultivated at a 1:1 ratio with the indicated CAR/4αβ-engineered T cells in the absence of exogenous cytokine, following ex vivo expansion and enrichment of CAR T cells using IL-4. Data show the mean ± SD of residual tumor cell viability from 3–12 independent replicates, quantified by MTT assay or by measuring luciferase activity at 24–72 hr. At each time point, percentage cell survival has been expressed relative to untreated tumor cells (set at 100% viability). H, high; I, intermediate; L, low; M, minimal/negative expression of αvβ6.

tumor cells, which naturally express this integrin (data not shown). Unlike control T cells, human A20-28z^{+} T cells destroyed 4T1 tumor cells, accompanied by the release of IFN-γ (Figure S9; data not shown).

We have shown previously that CAR T cells delivered using the i.p. route remain largely in the peritoneal cavity.[34] Nonetheless, they can trigger severe macrophage-dependent CRS, particularly in the presence of advanced tumor burden.[33] Such toxicity was not

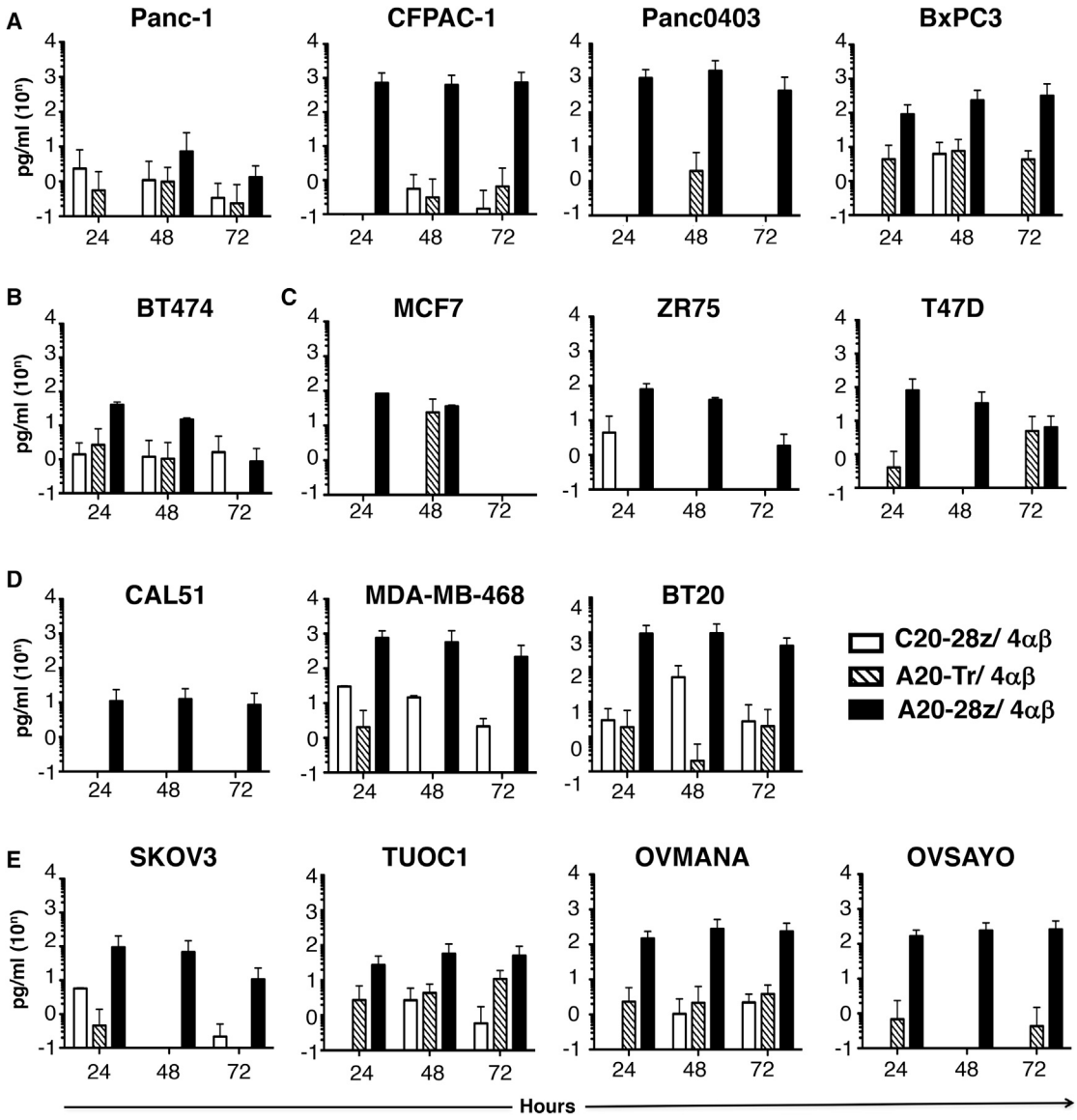

Figure 3. Production of IL-2 by αvβ6-Re-targeted CAR T Cells

Firefly luciferase-expressing pancreatic (A), HER2$^+$ breast (B), luminal breast (C), triple-negative breast (D), or ovarian tumor cells (E) were co-cultivated at a 1:1 ratio with the indicated CAR/4αβ-engineered T cells in the absence of exogenous cytokine, following ex vivo expansion and enrichment of CAR T cells using IL-4. Supernatant was harvested at each time point and analyzed for IL-2. Data show the mean ± SD of three to six independent replicates.

seen in the tumor xenograft models presented above. However, i.p. delivery may not permit human CAR T cells to access all sites where αvβ6 is naturally expressed in mice, notably gastrointestinal epithelium.[28] Consequently, we performed a study in which bolus doses of CAR T cells were administered intravenously (i.v.) to these animals. A single dose of 20×10^6 CAR T cells resulted in no weight loss or other clinical manifestations of toxicity. By contrast, when 40×10^6 A20-28z/4αβ$^+$ T cells were administered in two divided doses over 24 hr, significant weight loss was observed, which was transient and fully reversible. Toxicity was dependent on an intact CAR, since it was not observed with T cells that expressed the truncated A20-Tr control (Figure S10).

DISCUSSION

Aberrant expression of the epithelial-specific integrin αvβ6 is prevalent in several cancers.[11–16,18] The pro-invasive effect of αvβ6 is most graphically illustrated by its predominant expression at the infiltrating margin of the tumor mass.[11] By contrast, expression of this integrin is scarcely detectable in healthy human tissues,[17,22] rendering it a highly attractive candidate for immunotherapeutic targeting. Here

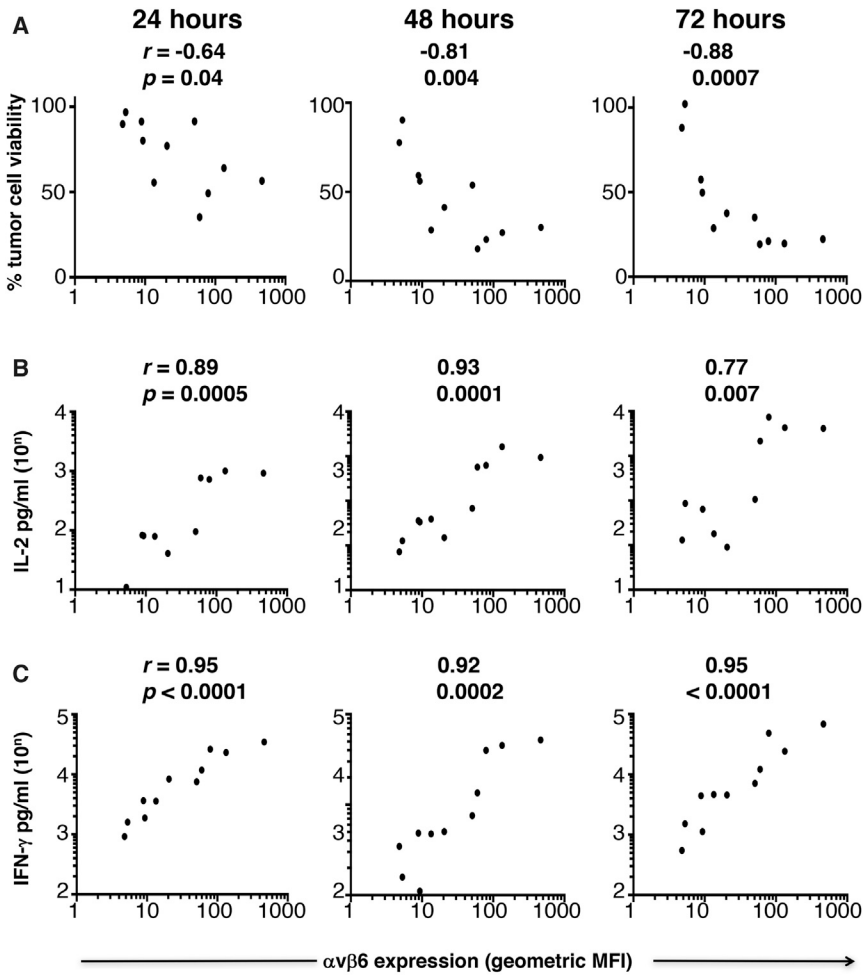

Figure 4. Relationship between Intensity of αvβ6 Integrin Expression by Tumor Cells and Effector Function of CAR T Cells

Expression of αvβ6 was determined by flow cytometry and then expressed as geometric mean fluorescence intensity (MFI), averaged over two to eight independent experiments. The relationships between MFI of αvβ6 on tumor cells and percentage tumor cell viability in cytotoxicity assays (A), release of IL-2 (B), and release of IFN-γ (C) by A20-28z/4αβ CAR T cells are depicted graphically, together with Pearson *r* correlation co-efficient and p (significance) values for each time point and effector parameter.

we show for the first time that T cells engineered to express an αvβ6-specific CAR mediate therapeutic activity against a broad range of solid tumor types, both in vitro and in vivo.

To engineer candidate αvβ6-targeted CAR T cells, two integrin-binding peptides were coupled to matched hinge, transmembrane, and CD28 + CD3ζ endodomain modules. The FMDV-derived A20 peptide has been characterized extensively for its ability to bind specifically to αvβ6, but not to other αv-based heterodimeric integrins. We found that T cells engineered to express an A20-derived CAR (A20-28z) killed tumor cell types of diverse origin, accompanied by cytokine release. Importantly, the magnitude of these effector activities correlated closely with cell surface expression of αvβ6 integrin, meaning that target cells with very low levels of αvβ6 (e.g., Panc-1 and CAL51) were ignored. We also evaluated an alternative second-generation CAR that was targeted using a 12-mer peptide, isolated by phage display.[29] The B12 peptide had been used to engineer a first-generation CAR to which some in vitro anti-tumor activity had been attributed.[35] However, this was demonstrated using a re-stimulated $CD8^+$ T cell line (isolated following hygromycin selection) and two derived $CD8^+$ T cell clones. When we re-evaluated this peptide in the context of a second-generation CAR that was expressed in unselected primary human T cells, negligible anti-tumor activity was observed. Given that the B12 peptide is shorter, it is possible that cognate epitope is not accessible by this very short peptide. Consequently, A20-28z alone was advanced for further study.

In vivo efficacy of A20-28z CAR T cells was demonstrated in four established xenograft models, representative of PDAC, breast, and ovarian cancers. Using a dual-BLI strategy, we demonstrated that αvβ6-re-targeted A20-28z$^+$ CAR T cells declined progressively in the days following delivery. This may account for the delayed tumor relapse observed, providing a rationale for the exploration of repeated T cell administration in future studies.[32]

Prior to adoptive transfer, genetically engineered T cells were enriched during ex vivo expansion since the CAR was co-expressed with 4αβ, a chimeric cytokine receptor that allows selective IL-4-mediated proliferation of CAR T cells.[31] This approach is now in use in a phase 1 clinical trial in patients with locally advanced or recurrent head and neck cancer. In that setting, a broadly reactive ErbB-specific CAR is co-expressed with 4αβ, allowing IL-4-mediated expansion of cell products prior to intra-tumoral delivery.[36] This approach obviates the need for leukapheresis, since over two billion CAR^+ T cells can reliably be expanded/enriched within 2 weeks from 120 mL blood, even from patients with advanced malignancy and profound lymphopenia. To date, eight CAR T cell batches have been produced in this ongoing trial that have exceeded these specifications, without any batch failures (data not shown).

In our study, we used the 4αβ system as a means of in vitro expansion. However, IL-4 also is produced in vivo in humans, and it may be

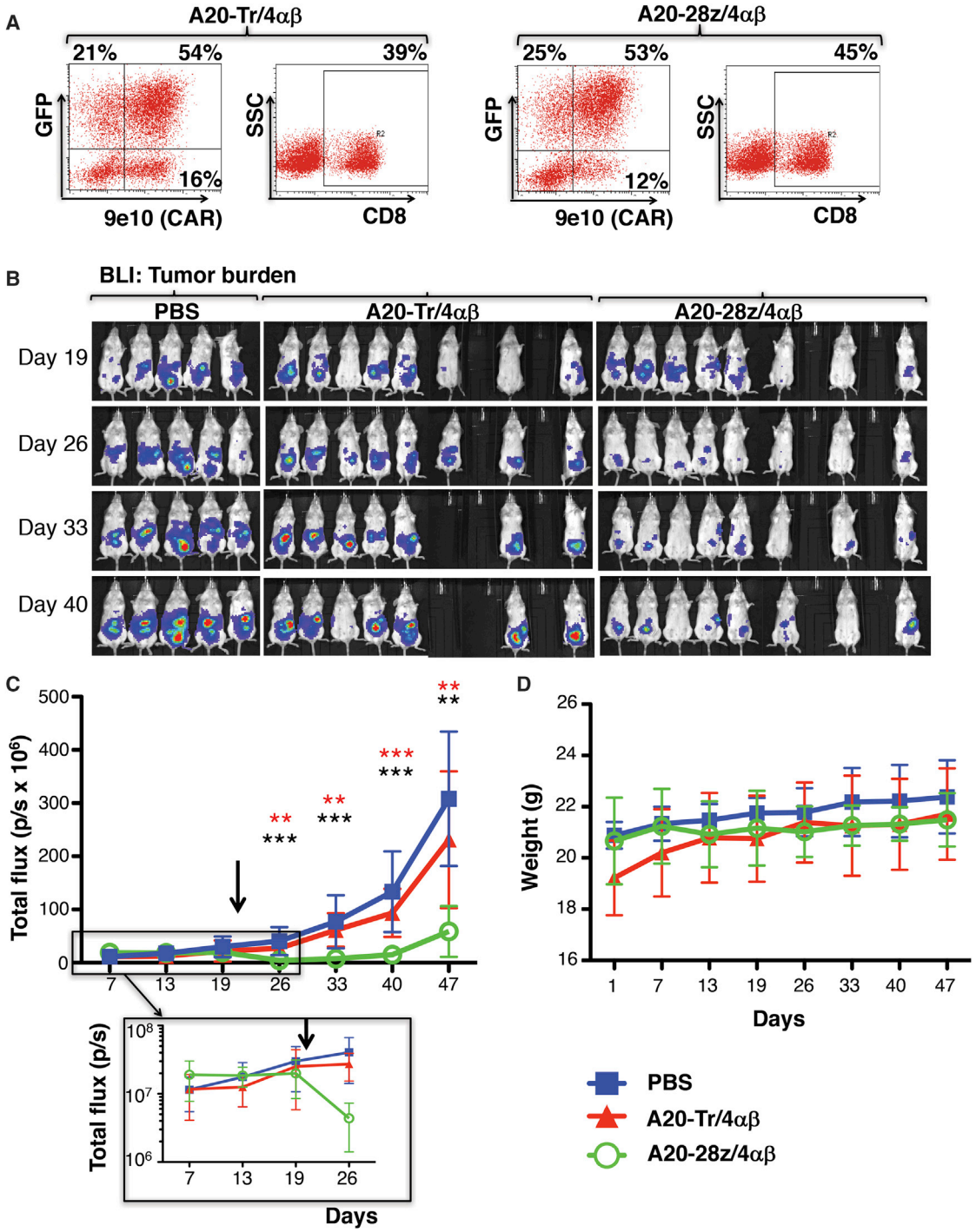

Figure 5. In Vivo Anti-tumor Activity of αvβ6-Re-targeted CAR T Cells against SKOV-3 Ovarian Tumor Xenografts

(A) T cells were co-transduced with retroviral vectors encoding for rluc/GFP and A20-28z/4αβ or the A20-Tr/4αβ truncated control. After culture for 12 days in IL-4, cells were analyzed by flow cytometry. 9e10 detects a myc epitope tag in the CAR ectodomain. SSC, side scatter. Quadrants were set using untransduced T cells cultured in IL-2. (B) Mice were injected i.p. with 1×10^6 SKOV-3-ffluc cells, and tumors were allowed to establish for 21 days before i.p. treatment with 10×10^6 of the indicated gene-modified T cells. Bioluminescence imaging using d-luciferin (substrate for ffluc) was used to monitor tumor status. (C) Data show the mean ± SD of tumor-derived total flux (n = 5–8 mice/group). Control mice received PBS. The arrow indicates the day of treatment with CAR T cells. The inset shows initial tumor regression on a log scale. $^{**}p < 0.01$; $^{***}p < 0.001$ (red, comparing A20-28z v PBS; black, comparing A20-28z v A20-Tr). (D) Mice were weighed weekly to assess toxicity of CAR T cells. Data show the mean ± SD of n = 5–8 mice/group. The arrow indicates the day of treatment with CAR T cells.

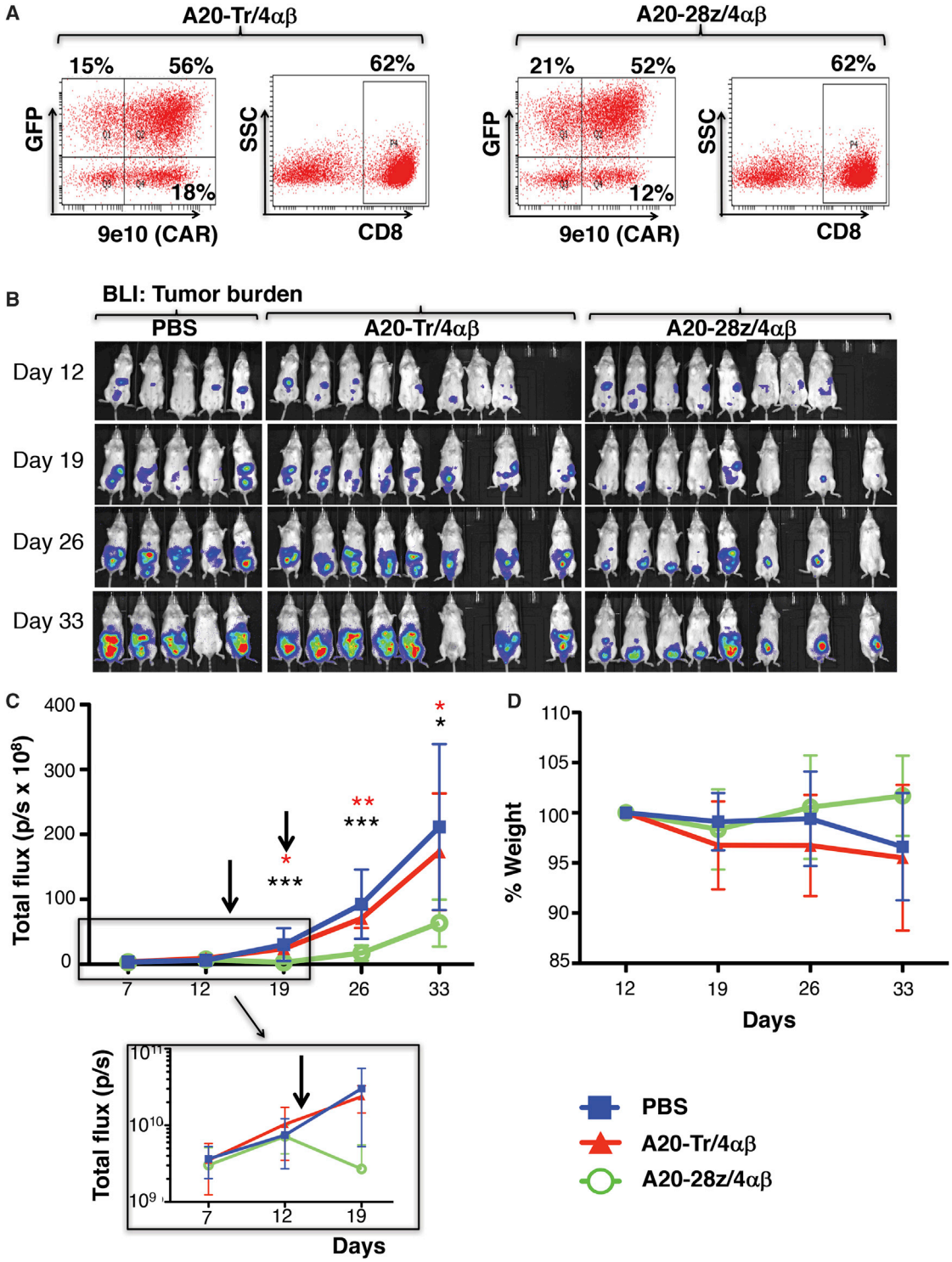

Figure 6. In Vivo Anti-tumor Activity of αvβ6-Re-targeted CAR T Cells against BxPC3 PDAC Xenografts

(A) T cells were co-transduced with retroviral vectors encoding for rluc/GFP and A20-28z/4αβ or the A20-Tr/4αβ truncated control. After culture for 12 days in IL-4, cells were analyzed by flow cytometry. 9e10 detects a myc epitope tag in the CAR ectodomain. SSC, side scatter. Quadrants were set using untransduced T cells cultured in IL-2.

(legend continued on next page)

overproduced in the tumor microenvironment. As discussed previously,[31] this could theoretically benefit anti-tumor activity but also might enhance the toxicity of this approach. In our study, we found that provision of exogenous IL-4 cytokine support did not improve anti-tumor activity of CAR T cells or their long-term survival. This may have been because of the very short half-life of IL-4 in vivo. Moreover, the combination IL-4 and CAR T cell treatment did not increase toxicity, although human IL-4 is not active in the mouse.

Meaningful safety testing of human A20-28z$^+$ CAR T cells could be undertaken in SCID beige mice for three reasons. First, the A20 FMDV-targeting moiety can bind to mouse αvβ6 integrin with comparable affinity to the human ortholog.[28] As a result, human A20-28z$^+$ CAR T cells also recognize mouse tumor cells that express this integrin. Second, we have shown previously that i.p. delivery of human ErbB-re-targeted CAR T cells can elicit severe CRS in SCID beige mice, in a manner that is accentuated by high tumor burden. In that setting, macrophage activation (a functionality that is preserved in SCID beige mice) accompanied by IL-6 release plays a pivotal role,[33] recapitulating the key role of these intermediates in human CRS.[37] Third, expression of αvβ6 in mice is proportionately greater than in man, most notably in the gastrointestinal tract.[28] In keeping with this, laboratory mice are highly susceptible to FMDV,[38] unlike man in which this viral illness is an extraordinarily unusual zoonosis.[39] Reassuringly, however, minimal toxicity accompanied tumor regression in all four xenograft models following treatment with αvβ6-targeted A20-28z CAR T cells. The administration of very large doses using the i.v. route did result in reversible toxicity, which was dependent upon an intact αvβ6-targeted CAR.

Taken together, these data justify the evaluation of αvβ6-targeted CAR T cell immunotherapy for tumors in which aberrant expression of this integrin is present. We are currently developing a strategy for phase 1 evaluation of this approach in patients with otherwise untreatable αvβ6-expressing malignancy.

MATERIALS AND METHODS

Retroviral Constructs

To enable detection of CARs, a myc epitope-tagged framework was engineered (Figures 1B–1D). A codon-optimized cDNA was synthesized to encode for human CD28 (amino acids 114–200) in which B7-binding residues 117–122 (MYPPPY) were substituted with residues 410–419 of human c-*myc* (EQKLISEEDL) (Mr Gene). The sequence was flanked by 5′ Not1 and 3′ Apa1 restriction sites and was substituted for the corresponding fragment in SFG T1E28z (encodes a broadly ErbB-reactive CAR with a CD28 + CD3ζ endodomain).[40] The resultant myc epitope-tagged CAR (Tm28z) exhibited comparable function to T1E28z (data not shown).

Next, codon-optimized cDNAs were synthesized in which two candidate αvβ6-binding peptide sequences were fused to signal peptides selected for correct cleavage site using SignalP 3.0 server[41] (Genscript; Figure 1A). The VP1-derived A20FMDV2 20-mer peptide was placed downstream of a CD124 signal peptide (A20).[42] A control (αvβ6 non-binding) peptide was generated in which the RGDL motif within A20FMDV2 was substituted with AAAA (C20). To engineer an alternative CAR-targeting moiety, a previously described αvβ6-binding 12-mer peptide (isolated by phage display)[29,35] was placed downstream of a human CD3γ signal peptide (B12) (Figure 1A). All cDNAs were substituted for the smaller Nco1/Not1 fragment within SFG Tm28z. The resultant CARs were named A20-28z, C20-28z, and B12-28z (Figure 1B). An endodomain-truncated control CAR (A20-Tr) also was engineered in which the Not1/Xho1 fragment within A20-28z was substituted with a smaller synthetic cDNA (Genscript) encoding CD28 residues 114–182 (in which MYPPPY was replaced by the myc epitope tag; Figure 1C).

In most experiments, CARs were co-expressed with an IL-4-responsive chimeric cytokine receptor (4αβ, in which the IL-4 receptor α ectodomain is fused to the shared transmembrane/endodomain of IL-2/15 receptor β; Figure 1D). T cells that express 4αβ undergo selective enrichment and expansion when cultured in IL-4.[31] Stoichiometric co-expression was achieved using an intervening furin cleavage site (RRKR), [serine-glycine]$_2$ linker, and *Thosea Asigna* 2A (T2A) peptide (Figure 1E).[31]

To visualize T cells in vivo, a red-shifted *Renilla reniformis* luciferase 8.6-535 (rluc; Genscript)[43] was co-expressed with GFP in a single SFG retroviral vector containing a furin cleavage site and T2A peptide (SFG rluc/GFP; Figure 1L). To visualize tumors in vivo, ffluc was co-expressed with tdTomato red fluorescent protein (tdRFP; Genscript) in a single SFG retroviral vector containing a furin cleavage site and T2A peptide (SFG ffluc/tdTom; Figure 1M).

Culture and Retroviral Transduction of Primary Human T Cells

Blood samples were obtained from healthy volunteers with approval of the South East London Research Ethics Committee 1 (reference 09/H0804/92). Activation of T cells was achieved 48 hr prior to gene transfer using CD3 + CD28-coated paramagnetic beads (1:1 bead: cell ratio; Thermo Fisher Scientific). Gene transfer was performed using PG13 retroviral packaging cells as described.[44] Transduced T cells were cultured in RPMI-1640 supplemented with 10% human AB serum (Sigma), GlutaMax, and antibiotic-antimycotic solution (Thermo Fisher Scientific) and in the presence of either 100 U/mL IL-2 (Proleukin, Novartis) or 30 ng/mL IL-4 (Gentaur).

(B) Mice were injected i.p. with 2×10^6 BxPC3-ffluc/tdTom cells, and tumors were allowed to establish for 14 days before i.p. treatment with 10×10^6 of the indicated gene-modified T cells. Bioluminescence imaging using d-luciferin (substrate for ffluc) was used to monitor tumor status. (C) Data show the mean ± SD of tumor-derived total flux (n = 5–8 mice/group). Control mice received PBS. The arrow indicates the day of treatment with CAR T cells. The inset shows initial tumor regression on a log scale. *$p < 0.02$; **$p < 0.004$; ***$p < 0.0001$ (red, comparing A20-28z v PBS; black, comparing A20-28z v A20-Tr). (D) Mice were weighed weekly to assess toxicity of CAR T cells. Data show the mean ± SD percentage body weight relative to pre-treatment of n = 5–8 mice/group. The arrow indicates the day of treatment with CAR T cells.

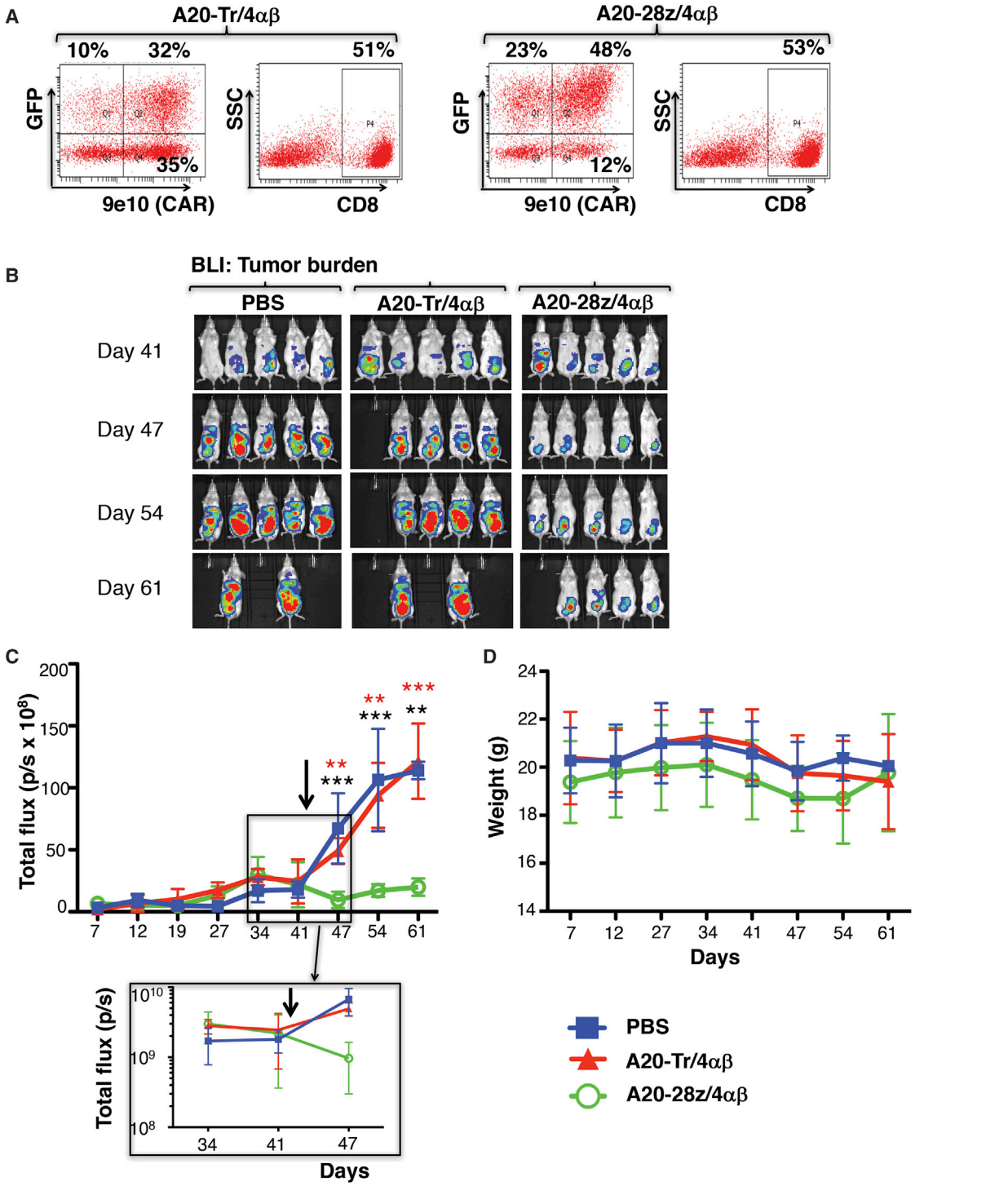

Figure 7. In Vivo Anti-tumor Activity of αvβ6-Re-targeted CAR T Cells against MDA-MB-468 Breast Cancer Xenografts

(A) T cells were co-transduced with retroviral vectors encoding for rluc/GFP together with A20-28z/4αβ or the truncated control, A20-Tr/4αβ. After culture for 12 days in IL-4, cells were analyzed by flow cytometry. 9e10 detects a myc epitope tag in the CAR ectodomain. SSC, side scatter. Quadrants were set using untransduced T cells cultured in IL-2. (B) Mice were injected i.p. with 2×10^6 MDA-MB468-ffluc cells, and tumors were allowed to establish for 42 days before i.p. treatment with 15×10^6 of the indicated

(legend continued on next page)

Cell Lines

Ffluc$^+$ Panc-1, BxPC3, ffluc$^+$ CFPAC1, ffluc$^+$ Panc0403, A375 puro (transduced with pBabe puro retrovirus), A375-β6 (transduced with pBabe puro retrovirus that encodes for human β6), A2780, A2780CP, and TOV21G cells were obtained from the Barts Cancer Institute, Queen Mary University of London. Ffluc$^+$ SKOV-3 cells were purchased from Caliper (PerkinElmer). Kuramochi and OVSAHO cells were obtained from the Japanese Collection of Research Bio-resources Cell Bank. The clear cell lines OVAS, SMOV2, KK, HAC2, OVTOKO, OVSAYO, TUOC1, and OVMANA were a kind gift from Dr. Itamochi, Tottori University School of Medicine. The breast cancer cell lines CAL51, BT20, MDA-MB-468, MCF7, BT474, and ZR75-1 were obtained from the Breast Cancer Now Research Unit, King's College London.

Tumor cell lines were grown in R10 or D10 medium, respectively comprising RPMI or DMEM (Lonza) supplemented with 10% fetal bovine serum (FBS, Sigma), GlutaMax, and antibiotic-antimycotic solution (Life Technologies). PG13 retroviral packaging cells were obtained from the European Collection of Cell Cultures (ECACC) and were maintained in D10. H29 retroviral packaging cells were a gift from Dr. Michel Sadelain (Memorial Sloan Kettering Cancer Center) and were propagated as described.[44] All tumor cell lines were validated by short-tandem-repeat DNA profiling, and experiments were performed within 30 passages of receipt.

Flow Cytometry Analysis

Expression of αvβ6 was detected using the 6.3G9 antibody,[45] followed by goat anti-mouse Ig-PE (Dako), and it was expressed as percentage positivity and/or geometric mean fluorescence intensity. Cells stained with secondary antibody only served as a negative control. Expression of CARs was detected using supernatant derived from the 9e10 hybridoma (ECACC), which binds to residues 410–419 of human c-*myc*, followed by goat anti-mouse Ig-PE. Untransduced T cells acted as a negative control. CD8 expression was detected using PE-conjugated PNIM0452 (Immunotech). Phenotypic analysis of T cells was performed using anti-CCR7 (R&D Systems, FAB197F) and CD45RO (BioLegend, 304210) antibodies. In some assays, populations were gated on CAR$^+$ cells detected using an antibody against CD124 (BD Pharmingen, 552178). To assess integrin specificity of the A20 peptide, biotinylated peptide (Genscript) was diluted in PBS supplemented with $MgCl_2$ and NaCl (Sigma, D8662) and incubated with cells on ice for 20 min before being stained with streptavadin-PE (LifeTech, S866) for a further 20 min on ice. Flow cytometry was performed using a FACSCalibur cytometer with CellQuest Pro software or Fortessa cytometer with FACSDiva software.

ELISA

Supernatants from tumor/T cell co-cultures were analyzed using a human IFN-γ or human IL-2 ELISA Ready-set-go kit (eBiosciences), as described by the manufacturer. To assess integrin specificity of the A20 peptide, ELISA plates were coated with recombinant αvβ6 (3817-AV-050), αvβ3 (3050-AV-050), αvβ5 (2528-AV-050), and αvβ8 (4135-AV-050) integrin proteins (all R&D Systems) in PBS overnight. Wells were washed with PBS supplemented with $MgCl_2$ and NaCl (wash buffer) before blocking for 2 hr with 1% w/v milk in wash buffer. After washing, 100 μL biotinylated peptide was added in 0.1% w/v milk in wash buffer for 1 hr, followed by washing and incubation with 100 μL 1:500 dilution streptavidin-HRP (Dako, P039701-2) for 1 hr. Plates were then washed and incubated with 100 μL hydrogen peroxide/tetramethylbenzidine (R&D Substrate Reagent DY999) for 20 min before the addition of 50 μL 2N sulphuric acid.

Cytotoxicity Assays

Tumor cell monolayers (96-well plate) were incubated with T cells for 24–72 hr at a 1:1 tumor cell:T cell ratio, unless otherwise indicated. Destruction of tumor cell monolayers by T cells was quantified using an MTT or luciferase assay. In the former, T cells were removed and MTT (Sigma) was added at 500 μg/mL in fresh D10 medium for 1–2 hr at 37°C and 5% CO_2. After removal of the supernatant, formazan crystals were re-suspended in 50 μL DMSO. Absorbance was measured at 560 nm. In luciferase assays, D-luciferin (PerkinElmer) was added at 150 μg/mL immediately prior to luminescence reading. Tumor cell viability was calculated as follows: (absorbance or luminescence of monolayer cultured with T cells/absorbance or luminescence of untreated monolayer alone) × 100%.

In Vivo Studies

All in vivo experimentation adhered to UK Home Office guidelines, as specified in project license number 70/7794, and it was approved by the King's College London animal welfare committee. Where necessary, tumor cells were transduced with SFG ffluc/tdTom and were purified by flow sorting prior to engraftment in vivo. SKOV-3 (1×10^6 cells), MDA-MB-468, Panc0403, or BxPC3 (2×10^6 cells each) were inoculated i.p. into SCID beige mice. Engineered T cells ($1–2 \times 10^7$ cells in total, as indicated in individual experiments) were administered i.p. on day 14 (BxPC3, Panc0403), day 21 (SKOV-3), or day 42 (MDA-MB-468). Bioluminescence imaging was performed using an IVIS Spectrum Imaging platform (PerkinElmer) with Living Image software (PerkinElmer). To image tumor status, mice were injected i.p. with D-luciferin (150 mg/kg; PerkinElmer) and imaged under isoflurane anesthesia after 12 min. To image T cells, mice were injected i.p. with coelenterazine (30 μg/mouse; PerkinElmer) and imaged under isoflurane anesthesia after 30 min. Image acquisition was conducted on a 15- or 25-cm field of view

gene-modified T cells. Bioluminescence imaging using d-luciferin (substrate for ffluc) was used to monitor tumor status. (C) Data show the mean ± SD of tumor-derived total flux (n = 5 mice/group). Control mice received PBS. The arrow indicates the day of treatment with CAR T cells. The inset shows initial tumor regression on a log scale. **$p < 0.003$; ***$p < 0.0003$ (red, comparing A20-28z v PBS; black, comparing A20-28z v A20-Tr). (D) Mice were weighed weekly to assess toxicity of CAR T cells. Data show the mean ± SD percentage body weight relative to pre-treatment of n = 5 mice/group. The arrow indicates the day of treatment with CAR T cells.

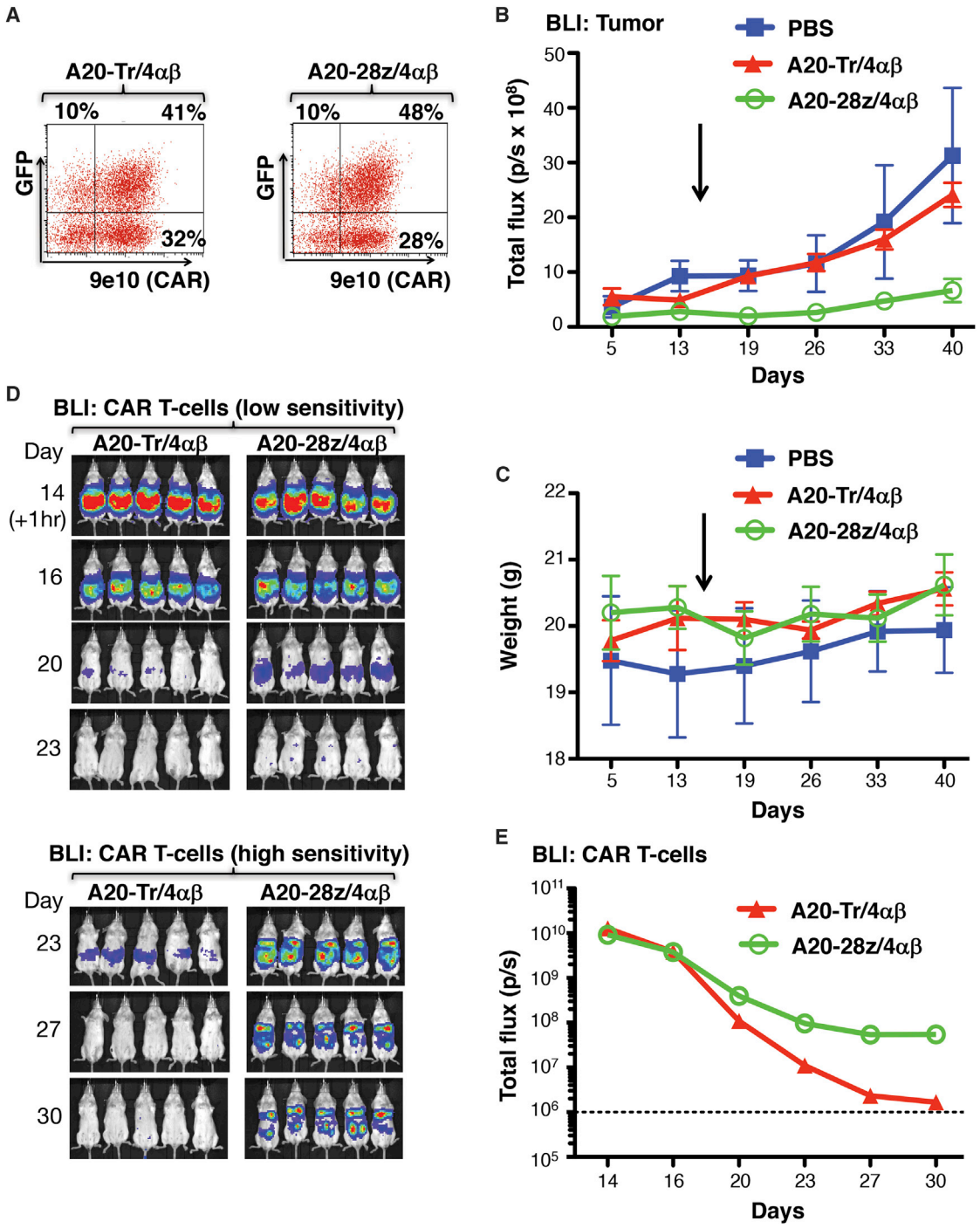

Figure 8. Imaging of Anti-tumor Activity and Persistence of αvβ6-Re-targeted CAR T Cells in SCID Beige Mice with Panc0403 PDAC Xenografts

(A) T cells were co-transduced with retroviral vectors encoding for rluc/GFP together with A20-28z/4αβ or the truncated control, A20-Tr/4αβ. After culture for 12 days in IL-4, cells were analyzed by flow cytometry. 9e10 detects a myc epitope tag in the CAR ectodomain. SSC, side scatter. Quadrants were set using untransduced T cells cultured in IL-2. (B) Mice were injected i.p. with 2×10^6 Panc0403-ffluc cells, and tumors were allowed to establish for 14 days before i.p. treatment with 10×10^6 of the indicated gene-modified T cells or PBS as control (arrow). Bioluminescence imaging using d-luciferin (substrate for ffluc) was used to monitor tumor status. Data show the mean ± SEM of tumor-derived total flux (n = 5 mice/group). (C) Mice were weighed weekly to assess toxicity of CAR T cells. Data show the mean ± SEM weight of n = 5 mice/group. To image T cells, BLI was performed after the administration of coelenterazine at the indicated intervals, commencing 1 hr after T cell injection. Images of individual mice (D) and pooled BLI data (E; mean ± SEM, n = 5) are shown.

with medium binning and auto-exposure. To assess safety of CAR T cells, i.v. bolus doses of 20 million CAR T cells were administered at the indicated intervals, making comparison with PBS. To assess the effect of exogenous 1×10^5 BxPC3 cells, they were inoculated i.p. into NSG mice before treatment with 2.5×10^6 T cells i.p. ± hIL-4 (Miltenyi). Interleukin-4 was administered three times weekly i.p. thereafter. In all experiments, animals were inspected daily and weighed weekly. Mice were culled if symptomatic as a result of tumor progression or weight loss of $\geq$20%.

Statistical Analysis

For comparison of two groups, datasets were analyzed using two-tailed Student's t test. Survival data were analyzed using the log-rank (Mantel-Cox) test. Correlation between the intensity of αvβ6 expression and T cell effector function was determined using Pearson *r* correlation. All statistical analysis was performed using GraphPad Prism version 5.0 or 6.0 or Excel for Mac 2011.

SUPPLEMENTAL INFORMATION

Supplemental Information includes ten figures and can be found with this article online at http://dx.doi.org/10.1016/j.ymthe.2016.10.012.

AUTHOR CONTRIBUTIONS

Conception and Design, J.M., J.F.M., and L.M.W.; Laboratory Work, L.M.W., A.C.P.-P., T.Z., D.M.D., R.M.G.P., Y.V.K., S.A.S., A.R., J.A.C.-G., and S. Vallath; Provision of Essential Materials and Advice, S. Violette, H.I., S.G.-M., and J.F.M.; Drafting of Manuscript, L.M.W. and J.M.; Critically Revising Manuscript, all authors.

CONFLICTS OF INTEREST

J.M. is chief scientific officer of Leucid Bio, which is a spinout company focused on the development of cellular therapeutic agents. There are no other conflicts of interest to disclose.

ACKNOWLEDGMENTS

This research was supported by Worldwide Cancer Research (13-1017), Breast Cancer Now (2010MayPR33), Pancreatic Cancer UK (A16648), King's Health Partners Confidence in Concept (MC_PC_14105), the Experimental Cancer Medicine Centre at King's College London, and by the National Institute for Health Research (NIHR) Biomedical Research Centre based at Guy's and St. Thomas' NHS Foundation Trust and King's College London. The views expressed are those of the authors and not necessarily those of the NHS, the NIHR, or the Department of Health. We thank Anthony Walker and Mike Garrison for useful discussions.

REFERENCES

1. Davila, M.L., Riviere, I., Wang, X., Bartido, S., Park, J., Curran, K., Chung, S.S., Stefanski, J., Borquez-Ojeda, O., Olszewska, M., et al. (2014). Efficacy and toxicity management of 19-28z CAR T cell therapy in B cell acute lymphoblastic leukemia. Sci. Transl. Med. *6*, 224ra25.
2. Maude, S.L., Frey, N., Shaw, P.A., Aplenc, R., Barrett, D.M., Bunin, N.J., Chew, A., Gonzalez, V.E., Zheng, Z., Lacey, S.F., et al. (2014). Chimeric antigen receptor T cells for sustained remissions in leukemia. N. Engl. J. Med. *371*, 1507–1517.
3. Kochenderfer, J.N., Dudley, M.E., Kassim, S.H., Somerville, R.P., Carpenter, R.O., Stetler-Stevenson, M., Yang, J.C., Phan, G.Q., Hughes, M.S., Sherry, R.M., et al. (2015). Chemotherapy-refractory diffuse large B-cell lymphoma and indolent B-cell malignancies can be effectively treated with autologous T cells expressing an anti-CD19 chimeric antigen receptor. J. Clin. Oncol. *33*, 540–549.
4. Morgan, R.A., Johnson, L.A., Davis, J.L., Zheng, Z., Woolard, K.D., Reap, E.A., Feldman, S.A., Chinnasamy, N., Kuan, C.T., Song, H., et al. (2012). Recognition of glioma stem cells by genetically modified T cells targeting EGFRvIII and development of adoptive cell therapy for glioma. Hum. Gene Ther. *23*, 1043–1053.
5. Johnson, L.A., Scholler, J., Ohkuri, T., Kosaka, A., Patel, P.R., McGettigan, S.E., Nace, A.K., Dentchev, T., Thekkat, P., Loew, A., et al. (2015). Rational development and characterization of humanized anti-EGFR variant III chimeric antigen receptor T cells for glioblastoma. Sci. Transl. Med. *7*, 275ra22.
6. Del Vecchio, C.A., Giacomini, C.P., Vogel, H., Jensen, K.C., Florio, T., Merlo, A., Pollack, J.R., and Wong, A.J. (2013). EGFRvIII gene rearrangement is an early event in glioblastoma tumorigenesis and expression defines a hierarchy modulated by epigenetic mechanisms. Oncogene *32*, 2670–2681.
7. Montano, N., Cenci, T., Martini, M., D'Alessandris, Q.G., Pelacchi, F., Ricci-Vitiani, L., Maira, G., De Maria, R., Larocca, L.M., and Pallini, R. (2011). Expression of EGFRvIII in glioblastoma: prognostic significance revisited. Neoplasia *13*, 1113–1121.
8. Morgan, R.A., Yang, J.C., Kitano, M., Dudley, M.E., Laurencot, C.M., and Rosenberg, S.A. (2010). Case report of a serious adverse event following the administration of T cells transduced with a chimeric antigen receptor recognizing ERBB2. Mol. Ther. *18*, 843–851.
9. Ahmed, N., Brawley, V.S., Hegde, M., Robertson, C., Ghazi, A., Gerken, C., Liu, E., Dakhova, O., Ashoori, A., Corder, A., et al. (2015). Human epidermal growth factor receptor 2 (HER2)-specific chimeric antigen receptor-modified T cells for the immunotherapy of HER2-positive sarcoma. J. Clin. Oncol. *33*, 1688–1696.
10. Hynes, R.O. (2002). Integrins: bidirectional, allosteric signaling machines. Cell *110*, 673–687.
11. Van Aarsen, L.A., Leone, D.R., Ho, S., Dolinski, B.M., McCoon, P.E., LePage, D.J., Kelly, R., Heaney, G., Rayhorn, P., Reid, C., et al. (2008). Antibody-mediated blockade of integrin alpha v beta 6 inhibits tumor progression in vivo by a transforming growth factor-beta-regulated mechanism. Cancer Res. *68*, 561–570.
12. Hazelbag, S., Kenter, G.G., Gorter, A., Dreef, E.J., Koopman, L.A., Violette, S.M., Weinreb, P.H., and Fleuren, G.J. (2007). Overexpression of the alpha v beta 6 integrin in cervical squamous cell carcinoma is a prognostic factor for decreased survival. J. Pathol. *212*, 316–324.
13. Elayadi, A.N., Samli, K.N., Prudkin, L., Liu, Y.H., Bian, A., Xie, X.J., Wistuba, I.I., Roth, J.A., McGuire, M.J., and Brown, K.C. (2007). A peptide selected by biopanning identifies the integrin alphavbeta6 as a prognostic biomarker for nonsmall cell lung cancer. Cancer Res. *67*, 5889–5895.
14. Moore, K.M., Thomas, G.J., Duffy, S.W., Warwick, J., Gabe, R., Chou, P., Ellis, I.O., Green, A.R., Haider, S., Brouilette, K., et al. (2014). Therapeutic targeting of integrin αvβ6 in breast cancer. J. Natl. Cancer Inst. *106*, dju169.
15. Ahmed, N., Riley, C., Rice, G.E., Quinn, M.A., and Baker, M.S. (2002). Alpha(v) beta(6) integrin-A marker for the malignant potential of epithelial ovarian cancer. J. Histochem. Cytochem. *50*, 1371–1380.
16. Sipos, B., Hahn, D., Carceller, A., Piulats, J., Hedderich, J., Kalthoff, H., Goodman, S.L., Kosmahl, M., and Klöppel, G. (2004). Immunohistochemical screening for beta6-integrin subunit expression in adenocarcinomas using a novel monoclonal antibody reveals strong up-regulation in pancreatic ductal adenocarcinomas in vivo and in vitro. Histopathology *45*, 226–236.
17. Thomas, G.J., Nyström, M.L., and Marshall, J.F. (2006). Alphavbeta6 integrin in wound healing and cancer of the oral cavity. J. Oral Pathol. Med. *35*, 1–10.
18. Bates, R.C., Bellovin, D.I., Brown, C., Maynard, E., Wu, B., Kawakatsu, H., Sheppard, D., Oettgen, P., and Mercurio, A.M. (2005). Transcriptional activation of integrin beta6 during the epithelial-mesenchymal transition defines a novel prognostic indicator of aggressive colon carcinoma. J. Clin. Invest. *115*, 339–347.
19. Thomas, G.J., Lewis, M.P., Whawell, S.A., Russell, A., Sheppard, D., Hart, I.R., Speight, P.M., and Marshall, J.F. (2001). Expression of the alphavbeta6 integrin

promotes migration and invasion in squamous carcinoma cells. J. Invest. Dermatol. *117*, 67–73.

20. Thomas, G.J., Lewis, M.P., Hart, I.R., Marshall, J.F., and Speight, P.M. (2001). AlphaVbeta6 integrin promotes invasion of squamous carcinoma cells through up-regulation of matrix metalloproteinase-9. Int. J. Cancer *92*, 641–650.
21. Morgan, M.R., Thomas, G.J., Russell, A., Hart, I.R., and Marshall, J.F. (2004). The integrin cytoplasmic-tail motif EKQKVDLSTDC is sufficient to promote tumor cell invasion mediated by matrix metalloproteinase (MMP)-2 or MMP-9. J. Biol. Chem. *279*, 26533–26539.
22. Breuss, J.M., Gallo, J., DeLisser, H.M., Klimanskaya, I.V., Folkesson, H.G., Pittet, J.F., Nishimura, S.L., Aldape, K., Landers, D.V., Carpenter, W., et al. (1995). Expression of the beta 6 integrin subunit in development, neoplasia and tissue repair suggests a role in epithelial remodeling. J. Cell Sci. *108*, 2241–2251.
23. Eberlein, C., Kendrew, J., McDaid, K., Alfred, A., Kang, J.S., Jacobs, V.N., Ross, S.J., Rooney, C., Smith, N.R., Rinkenberger, J., et al. (2013). A human monoclonal antibody 264RAD targeting αvβ6 integrin reduces tumour growth and metastasis, and modulates key biomarkers in vivo. Oncogene *32*, 4406–4416.
24. Kogelberg, H., Tolner, B., Thomas, G.J., Di Cara, D., Minogue, S., Ramesh, B., Sodha, S., Marsh, D., Lowdell, M.W., Meyer, T., et al. (2008). Engineering a single-chain Fv antibody to alpha v beta 6 integrin using the specificity-determining loop of a foot-and-mouth disease virus. J. Mol. Biol. *382*, 385–401.
25. Burman, A., Clark, S., Abrescia, N.G., Fry, E.E., Stuart, D.I., and Jackson, T. (2006). Specificity of the VP1 GH loop of Foot-and-Mouth Disease virus for alphav integrins. J. Virol. *80*, 9798–9810.
26. DiCara, D., Rapisarda, C., Sutcliffe, J.L., Violette, S.M., Weinreb, P.H., Hart, I.R., Howard, M.J., and Marshall, J.F. (2007). Structure-function analysis of Arg-Gly-Asp helix motifs in alpha v beta 6 integrin ligands. J. Biol. Chem. *282*, 9657–9665.
27. Hausner, S.H., DiCara, D., Marik, J., Marshall, J.F., and Sutcliffe, J.L. (2007). Use of a peptide derived from foot-and-mouth disease virus for the noninvasive imaging of human cancer: generation and evaluation of 4-[18F]fluorobenzoyl A20FMDV2 for in vivo imaging of integrin alphavbeta6 expression with positron emission tomography. Cancer Res. *67*, 7833–7840.
28. Saha, A., Ellison, D., Thomas, G.J., Vallath, S., Mather, S.J., Hart, I.R., and Marshall, J.F. (2010). High-resolution in vivo imaging of breast cancer by targeting the pro-invasive integrin alphavbeta6. J. Pathol. *222*, 52–63.
29. Kraft, S., Diefenbach, B., Mehta, R., Jonczyk, A., Luckenbach, G.A., and Goodman, S.L. (1999). Definition of an unexpected ligand recognition motif for alphav beta6 integrin. J. Biol. Chem. *274*, 1979–1985.
30. Maher, J., Brentjens, R.J., Gunset, G., Rivière, I., and Sadelain, M. (2002). Human T-lymphocyte cytotoxicity and proliferation directed by a single chimeric TCRzeta /CD28 receptor. Nat. Biotechnol. *20*, 70–75.
31. Wilkie, S., Burbridge, S.E., Chiapero-Stanke, L., Pereira, A.C., Cleary, S., van der Stegen, S.J., Spicer, J.F., Davies, D.M., and Maher, J. (2010). Selective expansion of chimeric antigen receptor-targeted T-cells with potent effector function using interleukin-4. J. Biol. Chem. *285*, 25538–25544.
32. Parente-Pereira, A.C., Whilding, L.M., Brewig, N., van der Stegen, S.J., Davies, D.M., Wilkie, S., van Schalkwyk, M.C., Ghaem-Maghami, S., and Maher, J. (2013). Synergistic chemoimmunotherapy of epithelial ovarian cancer using ErbB-retargeted T cells combined with carboplatin. J. Immunol. *191*, 2437–2445.
33. van der Stegen, S.J., Davies, D.M., Wilkie, S., Foster, J., Sosabowski, J.K., Burnet, J., Whilding, L.M., Petrovic, R.M., Ghaem-Maghami, S., Mather, S., et al. (2013). Preclinical in vivo modeling of cytokine release syndrome induced by ErbB-retargeted human T cells: identifying a window of therapeutic opportunity? J. Immunol. *191*, 4589–4598.
34. Parente-Pereira, A.C., Burnet, J., Ellison, D., Foster, J., Davies, D.M., van der Stegen, S., Burbridge, S., Chiapero-Stanke, L., Wilkie, S., Mather, S., and Maher, J. (2011). Trafficking of CAR-engineered human T cells following regional or systemic adoptive transfer in SCID beige mice. J. Clin. Immunol. *31*, 710–718.
35. Pameijer, C.R., Navanjo, A., Meechoovet, B., Wagner, J.R., Aguilar, B., Wright, C.L., Chang, W.C., Brown, C.E., and Jensen, M.C. (2007). Conversion of a tumor-binding peptide identified by phage display to a functional chimeric T cell antigen receptor. Cancer Gene Ther. *14*, 91–97.
36. van Schalkwyk, M.C., Papa, S.E., Jeannon, J.P., Guerrero Urbano, T., Spicer, J.F., and Maher, J. (2013). Design of a phase I clinical trial to evaluate intratumoral delivery of ErbB-targeted chimeric antigen receptor T-cells in locally advanced or recurrent head and neck cancer. Hum. Gene Ther. Clin. Dev. *24*, 134–142.
37. Maude, S.L., Barrett, D., Teachey, D.T., and Grupp, S.A. (2014). Managing cytokine release syndrome associated with novel T cell-engaging therapies. Cancer J. *20*, 119–122.
38. Salguero, F.J., Sánchez-Martín, M.A., Díaz-San Segundo, F., de Avila, A., and Sevilla, N. (2005). Foot-and-mouth disease virus (FMDV) causes an acute disease that can be lethal for adult laboratory mice. Virology *332*, 384–396.
39. Prempeh, H., Smith, R., and Müller, B. (2001). Foot and mouth disease: the human consequences. The health consequences are slight, the economic ones huge. BMJ *322*, 565–566.
40. Davies, D.M., Foster, J., Van Der Stegen, S.J., Parente-Pereira, A.C., Chiapero-Stanke, L., Delinassios, G.J., Burbridge, S.E., Kao, V., Liu, Z., Bosshard-Carter, L., et al. (2012). Flexible targeting of ErbB dimers that drive tumorigenesis by using genetically engineered T cells. Mol. Med. *18*, 565–576.
41. Bendtsen, J.D., Nielsen, H., von Heijne, G., and Brunak, S. (2004). Improved prediction of signal peptides: SignalP 3.0. J. Mol. Biol. *340*, 783–795.
42. Logan, D., Abu-Ghazaleh, R., Blakemore, W., Curry, S., Jackson, T., King, A., Lea, S., Lewis, R., Newman, J., Parry, N., et al. (1993). Structure of a major immunogenic site on foot-and-mouth disease virus. Nature *362*, 566–568.
43. Loening, A.M., Wu, A.M., and Gambhir, S.S. (2007). Red-shifted Renilla reniformis luciferase variants for imaging in living subjects. Nat. Methods *4*, 641–643.
44. Parente-Pereira, A.C., Wilkie, S., van der Stegen, S., Davies, D.M., and Maher, J. (2014). Use of retroviral-mediated gene transfer to deliver and test function of chimeric antigen receptors in human T-cells. J. Biol. Methods *1*, e7.
45. Weinreb, P.H., Simon, K.J., Rayhorn, P., Yang, W.J., Leone, D.R., Dolinski, B.M., Pearse, B.R., Yokota, Y., Kawakatsu, H., Atakilit, A., et al. (2004). Function-blocking integrin alphavbeta6 monoclonal antibodies: distinct ligand-mimetic and nonligand-mimetic classes. J. Biol. Chem. *279*, 17875–17887.

YMTHE, Volume *25*

Supplemental Information

Targeting of Aberrant αvβ6 Integrin Expression in Solid Tumors Using Chimeric Antigen Receptor-Engineered T Cells

Lynsey M. Whilding, Ana C. Parente-Pereira, Tomasz Zabinski, David M. Davies, Roseanna M.G. Petrovic, Y. Vincent Kao, Shobhit A. Saxena, Alex Romain, Jose A. Costa-Guerra, Shelia Violette, Hiroaki Itamochi, Sadaf Ghaem-Maghami, Sabari Vallath, John F. Marshall, and John Maher

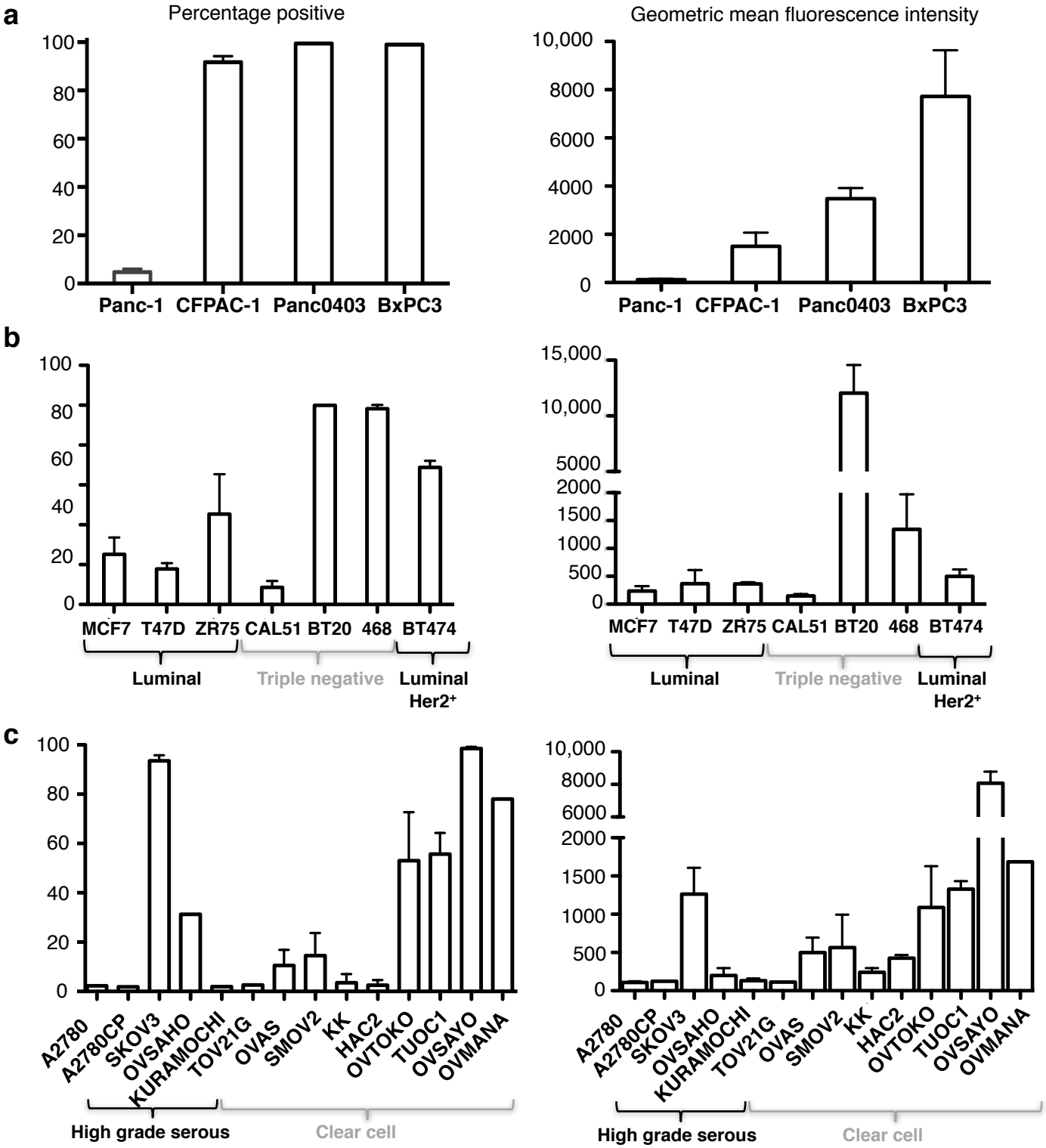

Supplementary Figure S1: Expression of αvβ6 integrin by tumor cell lines. Immortalized pancreatic (**a**), breast (**b**) and ovarian cancer cell lines (**c**) cells were analyzed for expression of the β6 integrin subunit by flow cytometry after incubation with the 6.3G9 antibody followed by goat anti-mouse IgG-PE. Cells stained with secondary antibody alone served as negative control. Data show the mean ± SD from 2-8 independent experiments.

Supplementary Figure S2

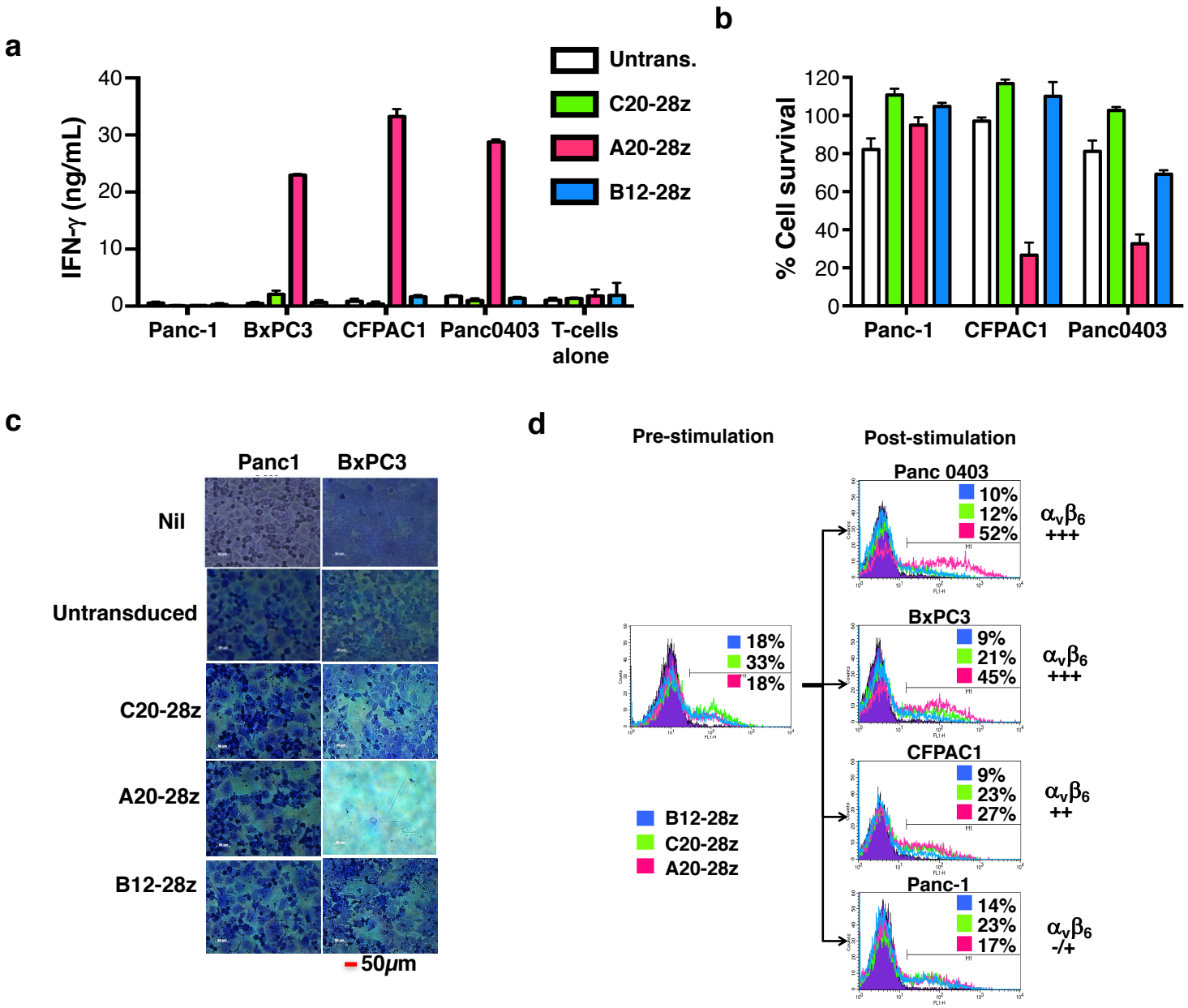

Supplementary Figure S2: *In vitro* comparison of anti-tumor activity of candidate αvβ6-specific CARs. (**a**) T-cells that expressed indicated CARs were co-cultivated at a 10:1 ratio with the specified pancreatic cell lines. After 24h, IFN-γ was measured in harvested supernatants while residual tumor cell viability was assessed by MTT assay (**b**). Both datasets show mean ± SD of 6 replicates. (**c**) 1 x 10^6 T-cells that expressed indicated CARs were co-cultivated with a confluent monolayer (24 well plate) of the indicated pancreatic tumor cell line, making comparison with untransduced T-cells or no addition (nil). After 24h, cultures were supplemented with IL-2 (100U/mL), which was added thereafter three times per week. Residual tumor monolayers were stained by crystal violet on day 8. (**d**) T-cells described in **c** were analyzed by flow cytometry for CAR expression before and after culture with the indicated monolayer for 8 days. Crystal violet and CAR T-cell enrichment data are representative of three independent cultures with αvβ6-expressing pancreatic tumor cell lines.

Supplementary Figure S3

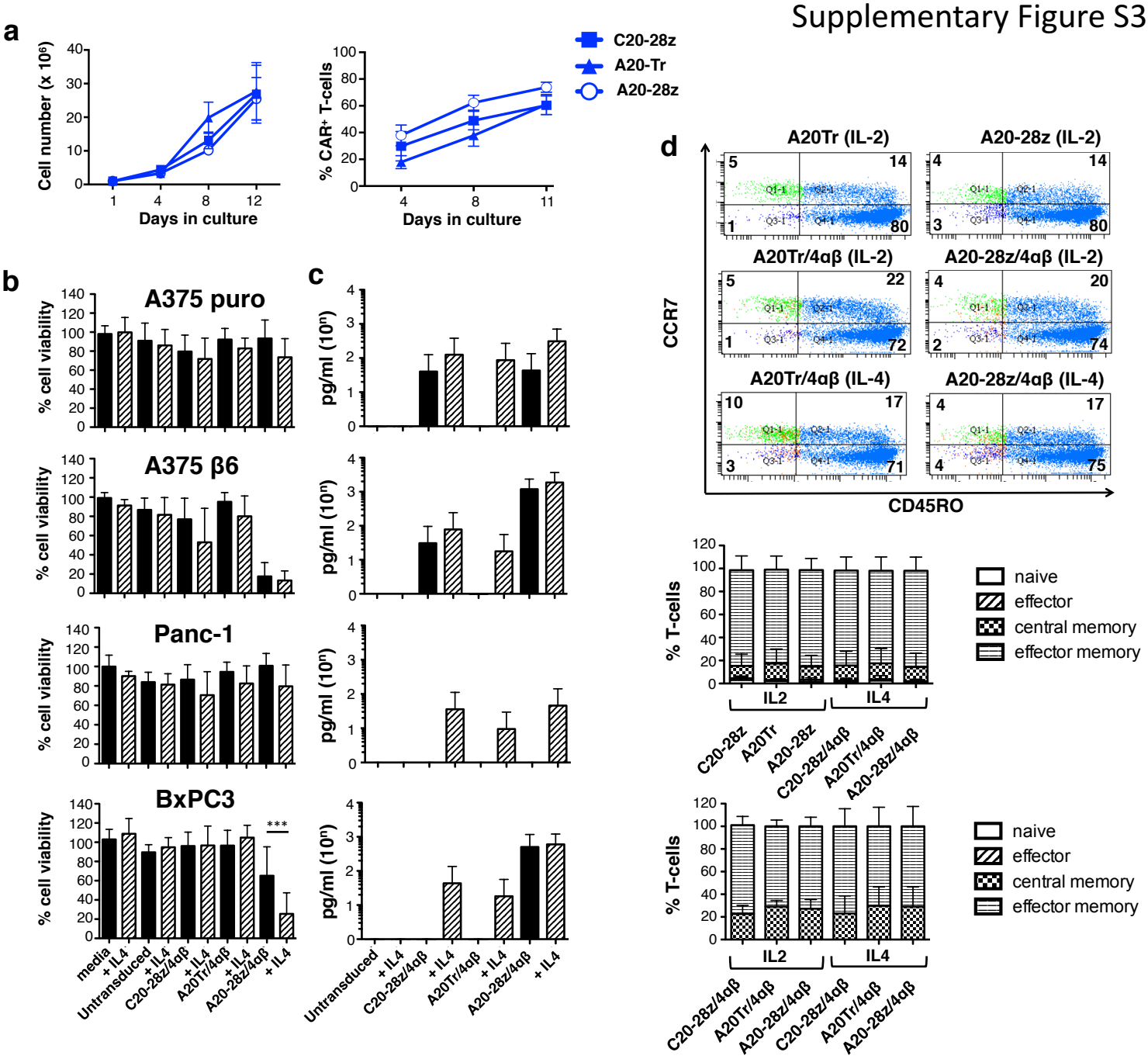

Supplementary Figure S3: Expansion and enrichment of CAR T-cells in IL-4. (a) Culture of 4αβ-expressing CAR T-cells in IL-4, demonstrating expansion and enrichment of the indicated CAR T-cell populations (mean ± SD, n=5-6 independent replicates). Tumour cells were co-cultivated at a 1:1 ratio with the indicated CAR/4αβ-engineered T-cells in the absence or presence of exogenous cytokine (30ng/ml), following *ex vivo* expansion and enrichment of CAR T-cells using IL-4. **(b)** Cytotoxicity and **(c)** IFN-γ release was analysed at 48hrs. Data show the mean mean ± SD of 5 independent experiments, each performed in triplicate. **(d)** The phenotype of T-cells cultured in either IL-2 or IL-4 for 12 days was assessed by flow cytometry. Data show representative plots and pooled data from T-cells derived from 5 independent donors.

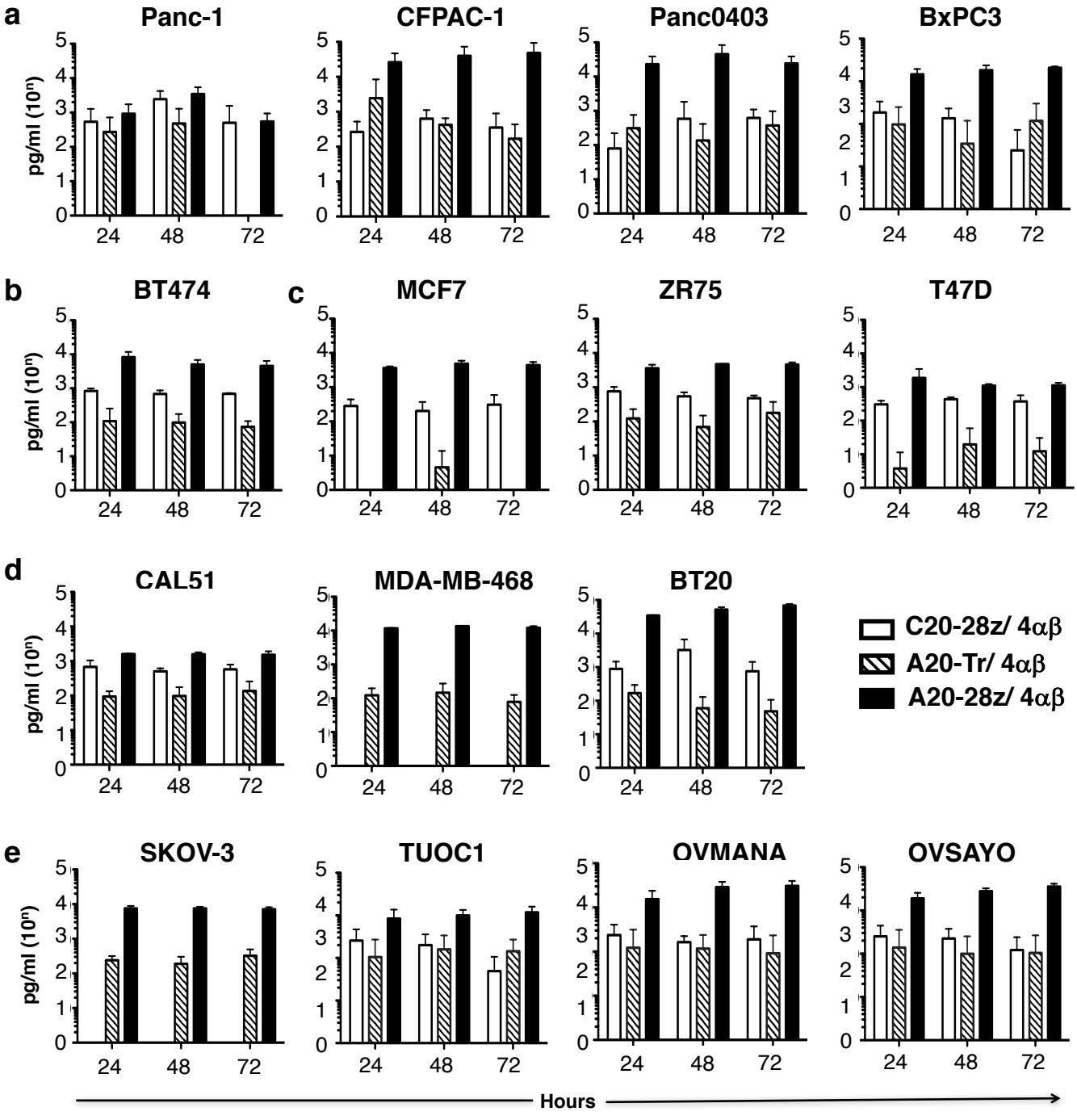

Supplementary Figure S4: Production of interferon (IFN)-γ by αvβ6 re-targeted CAR T-cells. Firefly luciferase-expressing pancreatic (**a**), HER2^{+} breast (**b**), luminal breast (**c**), triple negative breast (**d**), or ovarian tumor cells (**e**) were co-cultivated at a 1:1 ratio with the indicated CAR/4αβ-engineered T-cells in the absence of exogenous cytokine, following *ex vivo* expansion and enrichment of CAR T-cells using IL-4. Supernatant was harvested at each time-point and analyzed for IFN-γ. Data shows the mean ± SD of 3-6 independent replicates.

Supplementary Figure S5

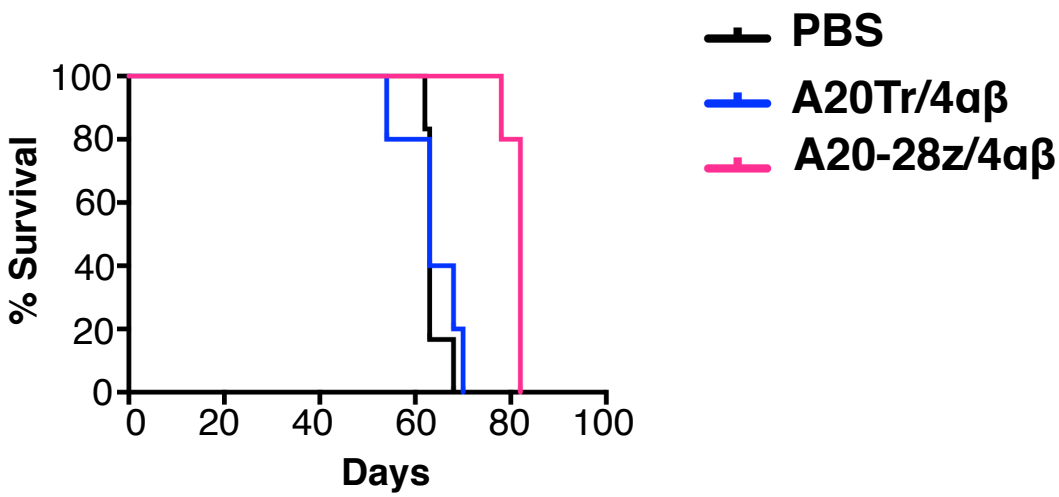

Supplementary Figure S5: Survival curve. Mice were injected i.p. with 1 x 10^6 SKOV-3-ffluc cells and tumors were allowed to establish for 21 days before i.p. treatment with 10 x 10^6 of the indicated gene-modified T-cells. Control mice received PBS. Animals were culled when humane endpoints were reached. p = 0.0014 comparing A20-28z/4$\alpha\beta$ treated mice with both other groups using the Log-rank (Mantel-Cox) test.

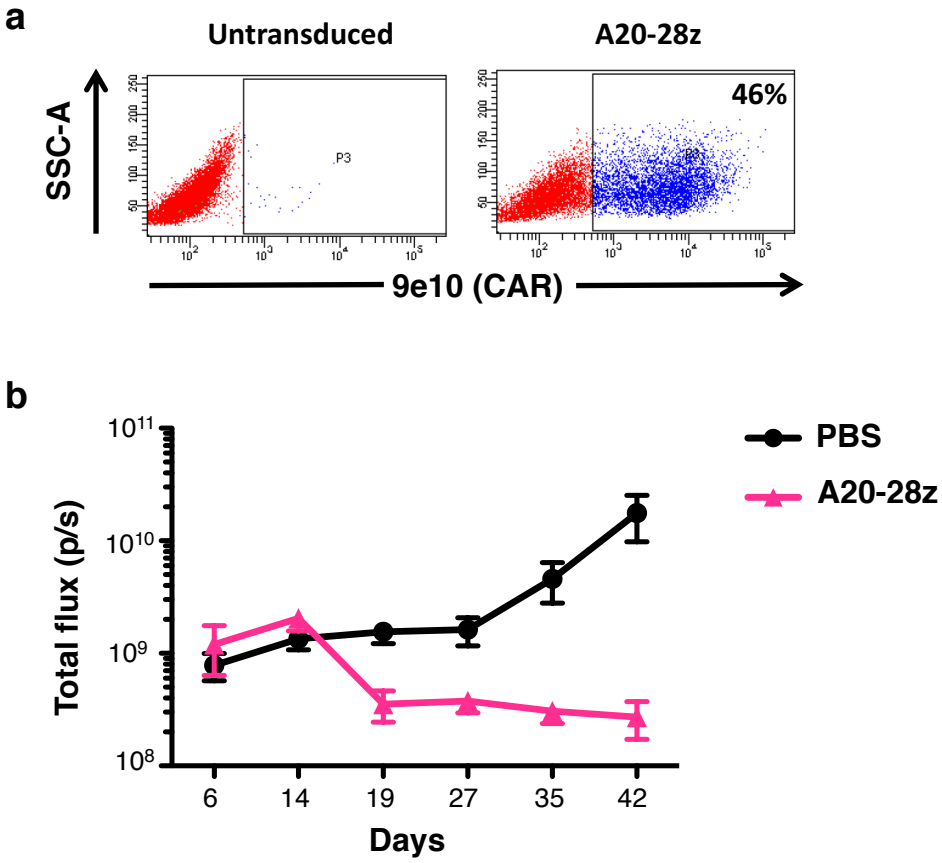

Supplementary Figure S6: *In vivo* anti-tumor activity of αvβ6 re-targeted CAR T-cells against Panc0403 PDAC xenografts. (**a**) T-cells were transduced with a retroviral vector encoding for A20-28z (e.g. without 4αβ). After culture for 6 days in IL-2, cells were analyzed by flow cytometry. 9e10 detects a myc epitope tag in the CAR ectodomain. SSC – side scatter. Gates were set using untransduced T-cells cultured in IL-2. (**b**) Mice were injected i.p. with 2 x 10^6 Panc0403-ffluc cells and tumors were allowed to establish for 14 days before i.p. treatment with 20 x 10^6 of A20-28z T-cells or PBS as control. Bioluminescence imaging using d-luciferin (substrate for ffluc) was used to monitor tumor status. Data show the mean ± SD of tumor-derived total flux (n=5 mice per group). The arrow indicates the day of treatment with CAR T-cells.

a

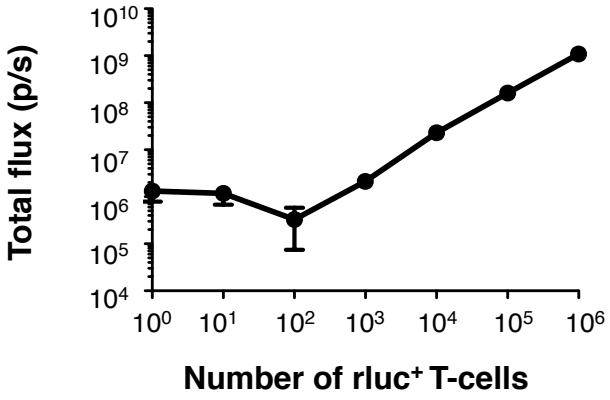

b

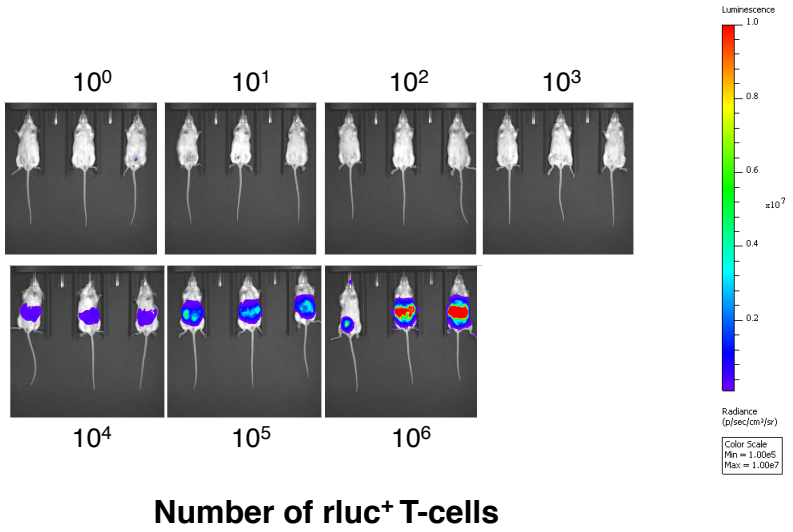

Supplementary Figure S7: *In vivo* imaging of adoptively transferred T-cells that express *Renilla* luciferase. (**a**) T-cells were transduced with a retroviral vector encoding rluc/GFP. The indicated number of rluc+ T-cells were injected i.p. into SCID-Beige mice, followed by i.p. injection of substrate (coelenterazine) and BLI imaging after 30 minutes. The graph shows the mean ± SD of 3 mice/group. Images of individual mice are shown in **(b).**

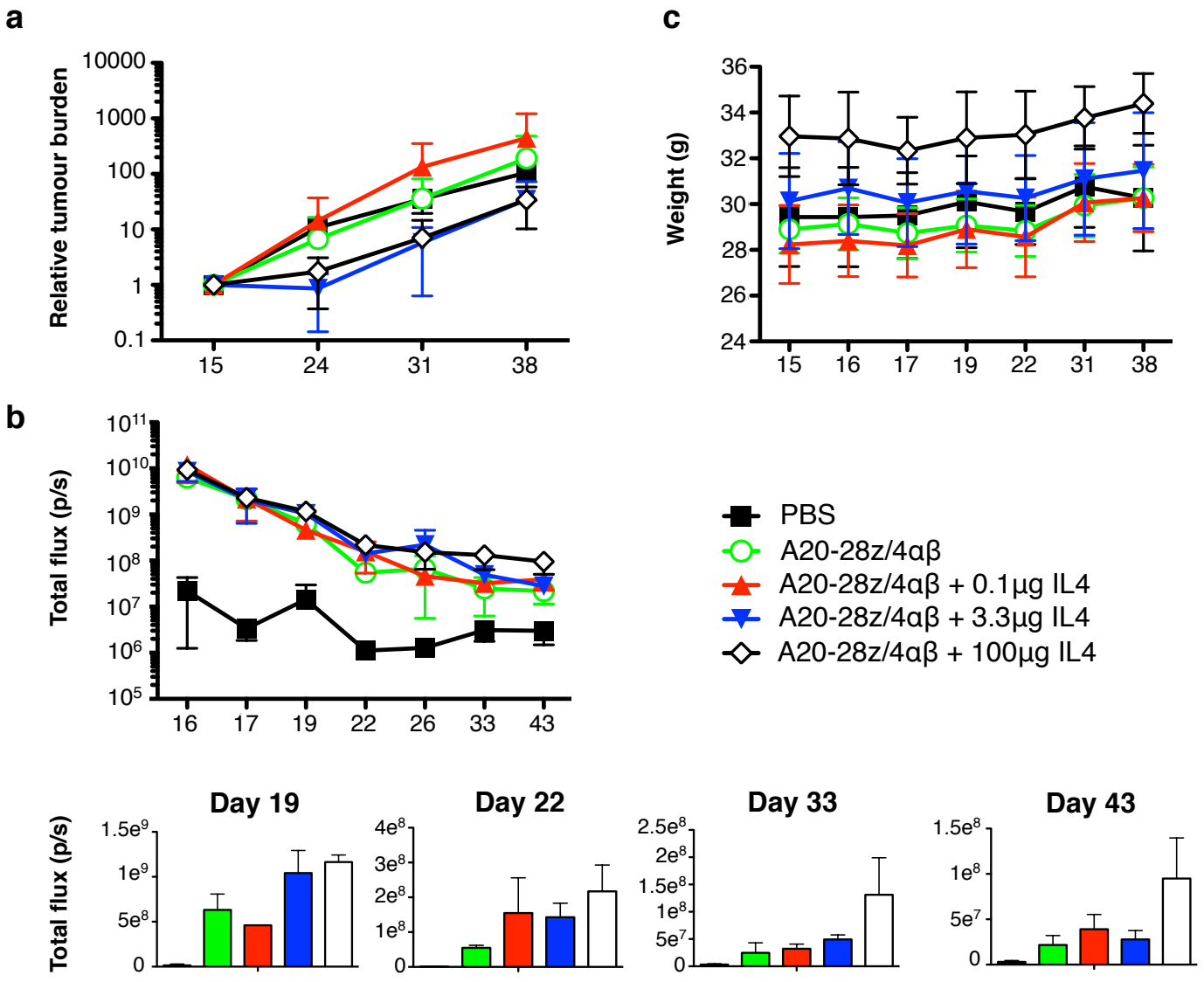

Supplementary Figure S8: Tumor stress test to evaluate effect of exogenous IL-4 treatment on T-cell activity *in vivo.* 1x10^5 BxPC3-ffluc cells were injected i.p. in NSG mice. Tumors were allowed to establish for 16 days prior to injection of 2.5 x 10^6 CAR T-cells i.p. Either PBS or the indicated dose of human IL-4 was administered 3 times per week thereafter using the i.p. route. T-cells were transduced with A20-28z/4αβ CAR and a retroviral vector encoding rluc/GFP to enable imaging of CAR T-cells. **(a)** Tumour burden was assessed weekly by BLI. Tumour burden is expressed relative to pre-treatment levels. **(b)** T-cells were imaged using coelenterazine administered i.p.. All data show the mean± SD of 3 mice/group. **(c)** Weight of mice during the study.

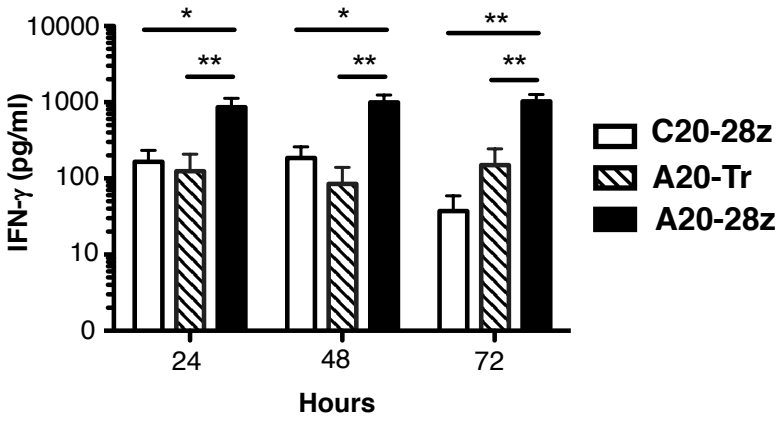

Supplementary Figure S9: Production of IFN-γ by αvβ6 re-targeted human CAR T-cells when stimulated by mouse tumor cells that naturally express αvβ6 integrin. 4T1 cells were co-cultivated at a 1:1 ratio with the indicated CAR/4αβ-engineered T-cells in the absence of exogenous cytokine, following *ex vivo* expansion and enrichment of CAR T-cells using IL-4. Supernatant was harvested at each time-point and analyzed for IFN-γ. Data shows the mean ± SD of 3 independent experiments, each performed in duplicate. * $p<0.05$; ** $p<0.01$.

Supplementary Figure S10

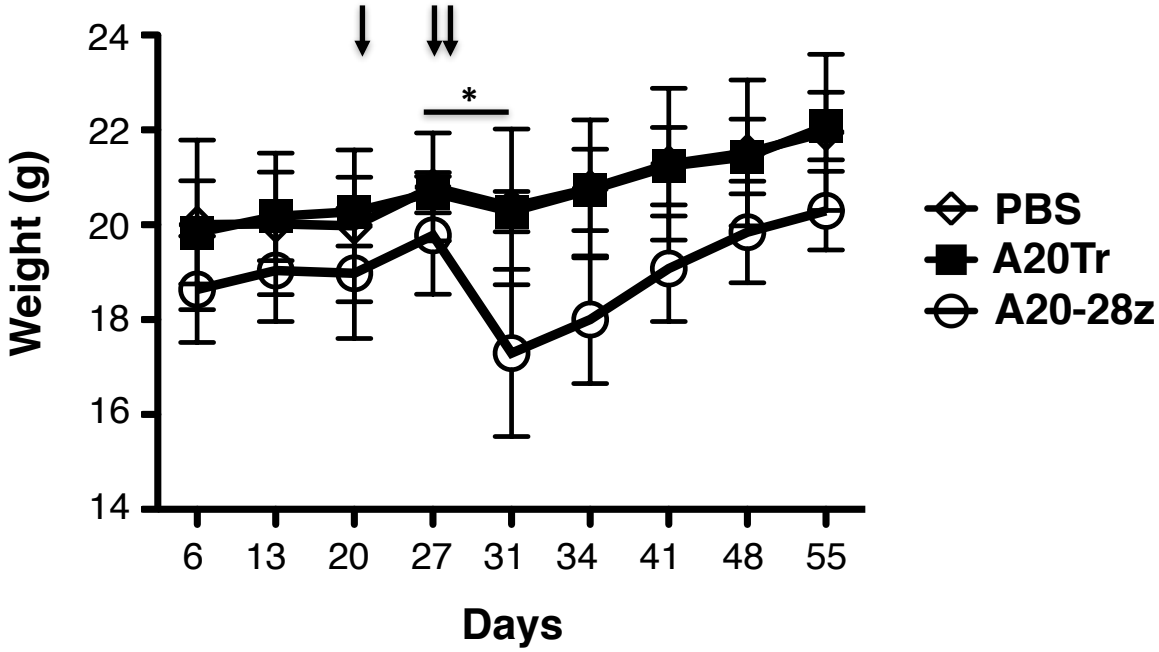

Supplementary Figure S10: *In vivo* safety testing of human αvβ6-retargeted CAR T-cells. SCID Beige mice received the indicated CAR T-cell populations that had been enriched to homogeneity following *ex vivo* culture in IL-4. Bolus doses of 20 million CAR T-cells were administered by iv (tail vein) injection at timepoints indicated by the overhead arrows. Animals were weighed at the indicated intervals (mean ± SD, n=5 mice per group). *p <0.05 for comparison of weight of A20-28z-treated mice on day 31 versus day 27.